IAI Journals.ASM.org

Establishment of Three *Francisella* Infections in Zebrafish Embryos at Different Temperatures

Espen Brudal,[a,b] Lilia S. Ulanova,[c] Elisabeth O. Lampe,[b,d] Anne-Lise Rishovd,[b,d] Gareth Griffiths,[c] Hanne C. Winther-Larsen[b,d]

Section for Microbiology, Immunology and Parasitology, Department of Food Safety and Infection Biology, Norwegian School of Veterinary Science, Oslo, Norway[a]; Laboratory for Microbial Dynamics[b] and School of Pharmacy,[d] University of Oslo, Oslo, Norway; Department of Biosciences, University of Oslo, Oslo, Norway[c]

***Francisella* spp. are facultative intracellular pathogens identified in increasingly diverse hosts, including mammals. *F. noatunensis* subsp. *orientalis* and *F. noatunensis* subsp. *noatunensis* infect fish inhabiting warm and cold waters, respectively, while *F. tularensis* subsp. *novicida* is highly infectious for mice and has been widely used as a model for the human pathogen *F. tularensis*. Here, we established zebrafish embryo infection models of fluorescently labeled *F. noatunensis* subsp. *noatunensis*, *F. noatunensis* subsp. *orientalis*, and *F. tularensis* subsp. *novicida* at 22, 28, and 32°C, respectively. All infections led to significant bacterial growth, as shown by reverse transcription-quantitative PCR (RT-qPCR), and to a robust proinflammatory immune response, dominated by increased transcription of tumor necrosis factor alpha (TNF-α) and interleukin-1β (IL-1β). *F. noatunensis* subsp. *orientalis* was the most virulent, *F. noatunensis* subsp. *noatunensis* caused chronic infection, and *F. tularensis* subsp. *novicida* showed moderate virulence and led to formation of relatively small granuloma-like structures. The use of transgenic zebrafish strains with enhanced green fluorescent protein (EGFP)-labeled immune cells revealed their detailed interactions with *Francisella* species. All three strains entered preferentially into macrophages, which eventually assembled into granuloma-like structures. Entry into neutrophils was also observed, though the efficiency of this event depended on the route of infection. The results demonstrate the usefulness of the zebrafish embryo model for studying infections caused by different *Francisella* species at a wide range of temperatures and highlight their interactions with immune cells.**

Members of the genus *Francisella* have been identified from many different environments and can infect and cause disease in diverse hosts, ranging from amoebae to humans (1, 2). *Francisella* species are nonmotile, pleomorphic, Gram-negative, strictly aerobic, facultative intracellular coccobacilli. The genus contains species capable of causing disease in humans (*F. tularensis* and *F. philomiragia*) as well as in fish (*F. noatunensis*) (2). *F. tularensis*, the causative agent of tularemia, is further divided into four subspecies, each with a distinct infectivity and capacity to cause illness in humans. Due to its extreme virulence, low infectious dose, ease of aerosol dissemination, and capacity to cause severe illness and death, *F. tularensis* subsp. *tularensis* has been classified as a class A bioterrorism agent by the Centers for Disease Control and Prevention (3). The closely related *F. tularensis* subsp. *novicida* has low virulence in humans but is highly infectious to mice and has been widely used as a model for *F. tularensis* (2). *F. noatunensis* subspecies are essentially avirulent to mammals (4) but cause francisellosis in fish (5), resulting in large losses for the fish farming industry worldwide (6–11). *F. noatunensis* consists of two subspecies, which appear to be adapted to different host temperatures: *F. noatunensis* subsp. *orientalis* causes disease in "warm-water" fish (6–9), while *F. noatunensis* subsp. *noatunensis* causes disease in fish living in colder waters (10–12).

Most *Francisella* spp. are highly infectious organisms for their hosts, where 10 to 30 CFU is capable of establishing infections (13–15), although the virulence of the strains differs. Infection with *F. tularensis* results in the development of tularemia, commonly characterized by the formation of localized or systemic suppurative (pus-forming) or granulomatous lesions (3), where the route of infection contributes significantly to the clinical symptoms. *F. noatunensis* subsp. *noatunensis* infection results in the development of chronic systemic granulomatous disease in Atlantic cod (11, 12), with cumulative mortality reaching 40% (11). *F. noatunensis* subsp. *orientalis* also causes systemic granulomatosis (7, 9, 16) with reported mortality of 50 to 60%.

An important part of *Francisella* sp. pathogenesis is the ability of the bacteria to replicate in the intracellular environment of professional phagocytic cells. For *F. tularensis* it has been shown that after phagocytosis by macrophages, the bacteria are able to lyse the phagosomal membrane and escape to the cytosol (17), where they replicate extensively (18). This eventually results in release of the bacteria to the extracellular space through host cell lysis or in the formation of *Francisella*-containing vacuoles through interactions with the autophagic pathway (19). It has been suggested that *F. noatunensis* subspecies are also able to escape from phagosomes into the cytosol (20–22).

In the early days of tularemia research, challenge experiments with human volunteers were performed. These studies provided valuable information regarding the efficacy of antibiotic treatment and vaccines (23–25), and some human studies are still being performed (26, 27). Several experimental models for studying tularemia are now available (23). The nonhuman primate model most closely resembles human tularemia with regard to strain

Received 24 January 2014 **Returned for modification** 18 February 2014
Accepted 27 February 2014
Published ahead of print 10 March 2014
Editor: R. P. Morrison
Address correspondence to Gareth Griffiths, g.w.griffiths@ibv.uio.no.
E.B. and L.S.U. contributed equally to this article.
Supplemental material for this article may be found at http://dx.doi.org/10.1128/IAI.00077-14.

doi:10.1128/IAI.00077-14

virulence and vaccine-induced protection (23). It is, however, not suitable as a standard model due to its high cost and public concern about the use of experimental animals. The mouse model has become popular for studying tularemia because of the wide availability of genetic tools. The use of the mouse model has its disadvantages, particularly with regard to susceptibility to different strains of *F. tularensis* and differences in vaccine-induced protection compared to the case for humans. While the rat model has gained some favor, especially in studying vaccine efficacy, it has reduced sensitivity to even the most virulent subspecies of *F. tularensis*. Thus, new infection models are warranted to fully understand *Francisella* infection and disease mechanisms.

F. noatunensis subsp. *orientalis* pathogenesis can be studied in its natural host Nile tilapia *Oreochromis niloticus* L., as it causes mortality in a dose-dependent manner within weeks after challenge (14). There have been several reports of tilapia being used for studying *F. noatunensis* subsp. *orientalis* virulence factors and vaccine efficacy (14, 28). The mortality of Atlantic cod challenged with *F. noatunensis* subsp. *noatunensis* under experimental conditions is highly variable, ranging from 75% (12) to a few percent, even many months after challenge, when gross pathology is evident in the fish (4, 29). Due to the slow progression of the disease, the inconsistent mortality of Atlantic cod, and the lack of alternate animal models (5), there is a need for establishment of models which allow faster development of the infection, giving more consistent results and hopefully providing insight into the *Francisella* sp. research in general. In addition, the above-mentioned models for studying francisellosis are not able to provide sufficient information about the initial steps of disease pathogenesis *in vivo*.

A large number of bacteria and viruses have been shown to cause disease in zebrafish (*Danio rerio*) (30, 31). Zebrafish has a number of valuable advantages compared to other commonly used models for studying *Francisella* pathogenesis. The fish are low cost, are easy to maintain, and require minimal laboratory space, in addition to the increasing availability of transgenic lines and a fully sequenced genome. The use of transparent zebrafish embryos infected with fluorescently labeled pathogens allows real-time *in vivo* imaging of disease progression, starting from the first minutes postinfection. The small size of adult zebrafish allows longitudinal histological sections to be made through the entire fish (30). Moreover, transgenic zebrafish lines with fluorescently labeled cells enable the study of the infected host cell repertoire. The embryological development of the zebrafish immune system also offers advantages (32). While the innate immune system, with its effector cells dominated by macrophages and neutrophilic granulocytes, is present and active within 48 h postfertilization (hpf), the adaptive arm of the immune system is not fully developed for another 4 to 6 weeks (33). This presents an opportunity to study the function of the innate immune system in a vertebrate host without the interference of adaptive immunity. The immune system of the fully immunocompetent zebrafish is closely related to those of other vertebrates, making zebrafish a more versatile model for studying pathogenesis and host-pathogen interactions than other nonmammalian models that lack an adaptive immune system, such as *Drosophila melanogaster* and *Caenorhabditis elegans* (30, 31).

Zebrafish have been shown to rapidly clear experimentally induced bacteremia within hours after infection with *Escherichia coli* K-12, *Bacillus subtilis*, and an avirulent strain of *Salmonella enterica* serovar Typhimurium (34, 35), suggesting a requirement for bacterial virulence to efficiently establish disease. The susceptibility of zebrafish to infection with *Francisella* was recently reported for *F. noatunensis* subsp. *orientalis* (36), in a study describing dose-dependent acute mortality of adult zebrafish upon intraperitoneal injections, demonstrating that *Francisella* can cause disease in adult zebrafish. Infected fish responded with a proinflammatory immune response characterized by increased transcription of interleukin-1β (IL-1β), gamma interferon (IFN-γ), and tumor necrosis factor alpha (TNF-α) starting at 6 h postinfection (hpi) and lasting at least 7 days. The study was done without the use of fluorescently labeled bacteria, and therefore no real-time observation of disease progression was provided. In the current study, we established and further characterized zebrafish embryo infection models for three different *Francisella* spp. at different temperatures.

MATERIALS AND METHODS

Strains, media, and growth conditions. The bacterial strains used in this study are given in Table S1 in the supplemental material. *F. noatunensis* subsp. *noatunensis* NCIMB14265, isolated from diseased Atlantic cod *Gadus morhua* L. in Norway, transformed with the green fluorescent protein (GFP)-expressing plasmid pKK289Km/*gfp* (*F. noatunensis* subsp. *noatunensis*-GFP) has been described previously as strain HWL108 (21). We additionally constructed a red fluorescent strain by transformation with the mCherry-expressing plasmid pKK289Km/*mCherry* (*F. noatunensis* subsp. *noatunensis*-mCh). *F. noatunensis* subsp. *orientalis* LADL 07-285A, isolated from diseased tilapia *Oreochromis* sp. L. in Costa Rica (16), was transformed with the mCherry-expressing plasmid pKK289Km/*mCherry* (*F. noatunensis* subsp. *orientalis*-mCh). *F. tularensis* subsp. *novicida* U112 was transformed with pKK289Km/*gfp* (*F. tularensis* subsp. *novicida*-GFP) and pKK289Km/*mCherry* (*F. tularensis* subsp. *novicida*-mCh). *E. coli* DH5α harboring the pmCherry vector (catalog no. 632522; Clontech Laboratories Inc., Mountain View, CA, USA) was used as a control in some experiments.

Bacteria were kept at −80°C for long-term storage either in BD Bacto Eugon broth (BD Diagnostic Systems, Sparks, MD, USA) supplemented with 20% glycerol (Sigma-Aldrich Co., St. Louis, MO, USA) or in autoclaved 10% skim milk (Merck KGaA, Darmstadt, Germany). Prior to experiments, bacteria were plated on Eugon chocolate agar (ECA) plates (37) supplemented with 15 μg/ml kanamycin (Sigma-Aldrich Co., St. Louis, MO, USA) and incubated at 22°C for *F. noatunensis* subsp. *noatunensis*, 28°C for *F. noatunensis* subsp. *orientalis*, and 37°C for *F. tularensis* subsp. *novicida*. *E. coli* pmCherry was propagated using Luria-Bertani agar with 50 μg/ml ampicillin (LAamp50). At 1 day prior to injections, the *Francisella* strains were inoculated into Eugon broth supplemented with 2 mM $FeCl_3$ (Sigma-Aldrich Co., St. Louis, MO, USA) and the appropriate concentration of kanamycin (15 μg/ml for *F. noatunensis* subsp. *orientalis* and *F. noatunensis* subsp. *noatunensis* and 30 μg/ml for *F. tularensis* subsp. *novicida*) and incubated overnight. *E. coli* pmCherry was grown overnight on LAamp50 plates and resuspended in phosphate-buffered saline (PBS) prior to injections.

Bacterial transformation with mCherry-expressing plasmid. The plasmid pKK289Km/*mCherry* was created by amplification of the *mCherry* gene from the pmCherry vector followed by ligation of the PCR product into the cloning vector pCR4 (Invitrogen by Life Technologies, Carlsbad, CA, USA), creating pCR4/*mCherry*. The resulting plasmid was digested with NdeI and EcoRI (New England BioLabs Inc., Ipswich, MA, USA) before the *mCherry* gene was ligated into the plasmid pKK289Km digested with the same enzymes, thereby placing the *mCherry* gene by translational fusion under control of the GroEL promoter. The plasmid was transformed into all *Francisella* strains by electroporation essentially as described by Bakkemo et al. (21).

Preparation of bacteria for microinjections. All the strains used for infecting zebrafish embryos expressed a fluorophore in *trans*, either GFP

or mCherry. Overnight cultures were harvested by centrifugation at 12,800 × *g* for 10 min at 4°C and the pellet resuspended in PBS, pH 7.4. Optical density at 600 nm (OD_{600}) was measured with a Genesys 20 spectrophotometer (Thermo Fisher Scientific Inc., Waltham, MA, USA) and adjusted to the desired value. An aliquot of phenol red sodium salt (Sigma-Aldrich Co., St. Louis, MO, USA) stock solution was added to the prepared bacterial suspensions in PBS to a final concentration of 0.01% to ensure visualization of the injection mixtures. The number of CFU per injection was estimated by plating 10 μl of 10-fold serial dilutions of the bacterial suspensions on ECA plates, which were incubated at the temperature optimal for each bacterial strain. The number of CFU was counted after at least 7 days for *F. noatunensis* subsp. *orientalis*, at least 3 weeks for *F. noatunensis* subsp. *noatunensis*, and 1 day for *F. tularensis* subsp. *novicida*.

Zebrafish embryo maintenance. Zebrafish (*Danio rerio*) wild-type (wt) strain AB embryos were obtained from the Aleström Zebrafish Lab facility at the Norwegian School for Veterinary Sciences. Transgenic zebrafish lines expressing enhanced GFP (EGFP) in macrophages [*Tg*(*mpeg1:EGPF*)*gl22*] (38) and neutrophilic granulocytes [*Tg*(*mpx*:EGFP)*i114*] (39) were kept at the Griffiths Zebrafish Lab at the University of Oslo, and embryos were produced in-house. All zebrafish adults and embryos were handled according to standard protocols (40). Zebrafish embryos were manually dechorionated at the age of 30 h, transferred into fresh embryo water, and kept at 28°C prior to injections.

Zebrafish embryo microinjections. Injections of zebrafish embryos were performed using a Narishige Inc. EG-400 microinjector with an Eppendorf Femtojet controlling unit. Borosilicate needles (Harvard apparatus, 1-mm outer diameter by 0.78-mm inner diameter) for the injections were prepared using a micropipette-pulling device (Shutter Inc., Flaming/Brown P-97) with the following parameters: heat, 610; pull, = 40; velocity, 5; and time, 5. The injection volume was adjusted by breaking the tip of an initially sealed needle at a certain point. Once the needle was opened, trial injections were made in paraffin oil, which led to the creation of droplets suspended in the oil. The diameter of the droplets was measured with a ruler incorporated into an eyepiece of the microscope, from which the injection volume was calculated. Different volumes were used for infection of the embryos at three anatomical sites (see Fig. S1 in the supplemental material): 2 to 3 nl for intravascular (duct of Cuvier), 1 to 2 nl for muscle tissue (tail muscle), and below 1 nl for the otic vesicle (ear). Wild-type strain AB or the transgenic zebrafish embryos at 48 to 52 h postfertilization (hpf) were anesthetized with approximately 170 μg/ml Tricaine methanesulfonate MS-222 (Tricaine) (pH 7.4) (Finquel; Argent Laboratories Group, Inc., Redmond, WA, USA) (41) for 1 to 2 min and placed on 2% agar (BD, Franklin Lakes, NJ, USA) plates before injection. Infected embryos were transferred into petri dishes with fresh embryo water and kept at 28°C for *F. noatunensis* subsp. *orientalis*, 22°C for *F. noatunensis* subsp. *noatunensis*, and 28°C or 32°C for *F. tularensis* subsp. *novicida*. Survival experiments were performed using at least 15 embryos per group injected with *Francisella* spp. in PBS with an OD_{600} of 2.0. PBS without bacteria was used for injections as negative controls. The survival data were processed using the Kaplan-Meier method with GraphPad Prism version 4.0 for Windows (GraphPad Software, La Jolla, CA, USA). For gene transcription studies, the group size was approximately 30 embryos to ensure a sufficient amount of genetic material.

Imaging of zebrafish embryos. Prior to imaging, zebrafish embryos were anesthetized with Tricaine as described above. Fluorescent imaging was performed with two light microscopes, the Leica DM IRB (Leica Microsystems CMS GmbH, Wetzlar, Germany) and Leica AF 6000 (Leica Microsystems AG, Heerbrugg, Switzerland). Confocal microscopy was performed with an Olympus Fluoview FV 1000 confocal microscope (Olympus Europa Holding GmbH, Hamburg, Germany). When using the Leica DM IRB inverted microscope, embryos were transferred to a glass slide with a reservoir filled with an anesthetic mixture of embryo water and Tricaine (see above) and covered with a coverslip. While using the Leica AF 6000, the embryos were transferred into a 47-mm petri dish filled with the mixture of embryo water and Tricaine. The embryos were anesthetized and embedded into low-melting-point agarose prior to confocal imaging. The micrographs were taken using Leica Application Suite (LAS) V3.8 and V4.0.0 and Olympus Fluoview version 3.1 software and further processed on the Fiji platform (42).

Sampling and RNA extraction from infected zebrafish embryos. At each time point, 9 randomly chosen zebrafish embryos (AB, wt) from each group were euthanized by a prolonged immersion in an overdose of Tricaine solution (200 to 300 μg/ml) (41) and transferred into 1.5-ml Eppendorf tubes. Three embryos were pooled into one sample to allow for a sufficient amount of starting material for RNA extraction, and the total number of samples per time point per strain was three. The embryo water was replaced by RNAlater (Ambion by Life Technologies, Carlsbad, CA, USA) immediately after transfer. The samples were kept at 4°C until extraction of RNA. For the extraction of total RNA, RNAlater was replaced with 1 ml of TRIzol (Ambion by Life Technologies, Carlsbad, CA, USA), the embryos were transferred together with the TRIzol to a 2.0-ml SafeLock Eppendorf tube (Eppendorf AG, Hamburg, Germany) containing a 0.5-mm-diameter steel bead (Qiagen GmBH, Hilden, Germany), and the tissue was homogenized at 25 Hz for 5 min with TissueLyserII (Qiagen GmBH, Hilden, Germany). After 5 min of incubation at room temperature, 200 μl chloroform (Sigma-Aldrich Co., St. Louis, MO, USA) was added, and the samples were incubated for 3 min at room temperature before centrifugation at 21,500 × *g* for 20 min at 4°C. RNA-containing supernatant was mixed with an equal volume of 70% ethanol and loaded on RNeasy Minispin columns (Qiagen GmBH, Hilden, Germany). The samples were thereafter handled according to the manufacturers' instructions, including a 15-min on-column DNase treatment using the RNase-free DNase set (Qiagen GmBH, Hilden, Germany), and eluted in 50 μl diethyl pyrocarbonate (DEPC)-treated H_2O (Invitrogen by Life Technologies, Carlsbad, CA, USA).

RNA quantity and quality were assessed as previously described (37). Due to a too-low concentration of RNA extracted from each pool of zebrafish embryos, we could not use 1 μg of RNA for reverse transcription (RT). The maximum amount of 12 μl RNA per reverse transcription reaction mixture (usually corresponding to between 300 and 600 ng total RNA), was therefore used for the reverse transcription step performed with QuantiTect the reverse transcription kit (Qiagen GmBH, Hilden, Germany) using random primers. A control experiment with reverse transcriptase omitted was performed for each extraction to investigate the potential presence of contaminating genomic DNA.

Primer design and quantitative PCR. Primers (see Table S2 in the supplemental material) were chosen to target a diverse repertoire of the immune response from zebrafish. TNF-α, IL-1β, and IL-12a were chosen to represent proinflammatory cytokines, as they are among the main proinflammatory cytokines produced by phagocytes (43). IL-10 (44) was chosen as an anti-inflammatory cytokine. Complement component 3b (C3b) was chosen to represent the complement system in zebrafish (45). IFN-γ1-2 was chosen for investigation of a potential type II interferon (IFN) response in zebrafish (46). Mx was chosen to represent genes induced by the type I IFNs in zebrafish (47). Suppressors of cytokine signaling (SOCS) were chosen due to their importance in regulation of the balance between pro- and anti-inflammatory signals during infection (48).

QuantiTect bioinformatically validated primers were obtained from Qiagen GmBH (Hilden, Germany) for most of the genes used in the study, while for the remaining immune genes, primers previously used in gene transcription studies of zebrafish (49) were obtained from Life Technologies Inc. (Carlsbad, CA, USA). Quantitative PCR (qPCR) was performed in triplicates using a LightCycler 480 (Roche, Basel, Switzerland) qPCR machine in 20-μl reaction volumes containing LightCycler 480 SYBR green I Master Mix (Roche, Basel, Switzerland), 0.5 μM each primer, and 2 μl template under the following cycling conditions: 5 min of initial denaturation at 95°C; 45 cycles of amplification using 10 s at 95°C, 30 s at 60°C, and 8 s at 72°C; and then melting curve analysis to verify single

amplification peaks for the immune response experiments. For quantification of bacterial growth, a Stratagene Mx3005p (Stratagene, La Jolla, CA) qPCR machine was used and the reactions run in triplicate in 20-μl volumes using Express SYBR GreenER qPCR Supermix Universal (Life Technologies Inc., Carlsbad, CA, USA) containing 50 nM Rox reference dye and 300 nM appropriate primers under the following cycling conditions: 2 min of incubation with uracil-DNA glycosylase (UDG) at 50°C, 2 min of initial denaturation at 95°C, 40 cycles of amplification using 15 s at 95°C and 60 s at 60°C, and melting curve analysis.

Relative transcription levels for each gene and time point were determined as previously described (37) and normalized against the reference genes *18S rRNA* (alternative designation, *zgc:158463*), *eef1a1l1*, and *actb1*, which have been previously reported to be stably transcribed during zebrafish embryonic development (50, 51). The normalized immune response data for infected fish were standardized against the transcription levels in PBS-injected fish for each time point, as the basal transcription levels of immune genes in PBS-injected fish depend on the stage of embryonic development (data not shown). Statistical analysis of the resulting data sets was performed using JMP 8.0.2. (SAS Institute Inc., Cary, NC, USA). Differences between groups were deemed statistically significant at a P value of <0.05 using Student's t test assuming unequal variance with a two-tailed test for the immune response and a one-tailed test for verification of bacterial growth.

The *gyrA* and the *fopA* genes were chosen for relative quantification of *F. noatunensis* subsp. *orientalis* and *F. noatunensis* subsp. *noatunensis*, respectively, as they have previously been used for RT-qPCR studies and were proved to be stably transcribed under various conditions (37). The *fopA* gene has additionally been used for diagnostic purposes (52) and was chosen for quantifying relative transcription levels for *F. tularensis* subsp. *novicida*.

RESULTS

Estimation of challenge dose. The amount of bacteria injected into the zebrafish embryos was controlled by OD_{600} measurements of the bacterial cultures in phosphate-buffered saline (PBS), which were subsequently used for infection. Plating *F. noatunensis* suspensions with an OD_{600} of 2.0 resulted in an estimated CFU count of 3.5×10^9 CFU/ml, corresponding to a challenge dose of approximately 9×10^3 CFU per embryo. Plating *F. tularensis* subsp. *novicida* suspensions with an OD_{600} of 2.0 in PBS gave an average count of 1.25×10^{10} CFU/ml, or approximately 3.3×10^4 CFU per embryo. The maximum amount of *F. tularensis* subsp. *novicida* used for infecting zebrafish embryos was therefore 3.6-fold higher than the corresponding doses of *F. noatunensis* subsp. *orientalis* and *F. noatunensis* subsp. *noatunensis*.

Model 1, infection of zebrafish embryos with *F. noatunensis* subsp. *orientalis* at 28°C: *F. noatunensis* subsp. *orientalis*-mCh infection causes acute disease and fast mortality in zebrafish embryos. Taking into consideration that *F. noatunensis* subsp. *orientalis*-mCh has the most favorable optimal growth temperature for the fish (28°C) and that adult zebrafish have previously been shown to be susceptible to *F. noatunensis* subsp. *orientalis* infection (36) *F. noatunensis* subsp. *orientalis*-mCh was the first strain tested for zebrafish embryo infection. Zebrafish embryos (AB, wild type [wt]) at 28°C were injected with 2 to 3 nl of *F. noatunensis* subsp. *orientalis*-mCh suspension at an OD_{600} of 2.0, 0.2, or 0.02 into the duct of Cuvier, a wide blood vessel that spreads over the top of the yolk sac (see Fig. S1 in the supplemental material). The bacteria were able to establish infection and kill all the infected embryos within 5 days postinfection (dpi) with a challenge dose at an OD_{600} of 2.0 or 0.2, while an OD_{600} of 0.02 resulted in only around 20% mortality (Fig. 1A). The ability of the bacteria to replicate inside the embryos was next evaluated by RT-qPCR (Fig. 1B). Bacterial RNA was detected in the infected embryos at all investigated time points, and the amount of *F. noatunensis* subsp. *orientalis*-mCh increased by 8-fold by 24 h postinfection (hpi) and by 23-fold by 48 hpi. This verified strong *F. noatunensis* subsp. *orientalis*-mCh growth in the infected embryos, with an estimated doubling time of 9 h.

(i) Imaging of *F. noatunensis* subsp. *orientalis*-mCh-infected zebrafish embryos reveals formation of granuloma-like structures. The first clinical sign of infection was decreased fish motility, usually on day 1 to 2 postinfection. Within hours after infection, we observed accumulation of fluorescently labeled bacteria by fluorescence microscopy. More detailed observation revealed fluorescent bacterial aggregates that enlarged over the course of the infection and were often visible in the infected embryos at late stages of the disease as what we operationally define as granuloma-like structures (GLS) (Fig. 1C). The GLS-containing red fluorescent bacteria formed rapidly and expanded.

(ii) Zebrafish embryo immune response to *F. noatunensis* subsp. *orientalis*-mCh infection. To investigate the immune response of zebrafish embryos to *F. noatunensis* subsp. *orientalis*-mCh infection, we used RT-qPCR to monitor the transcription of mRNA for selected immune-related genes. Single amplification peaks were obtained from all primer sets, and the absence of contaminating genomic DNA was verified using controls without reverse transcriptase. As summarized in Fig. 1D and shown in Fig. S2 in the supplemental material, the immune response was dominated by increased transcription of *il1b* and *tnfa*. Several pathogens, including *Francisella*, utilize the suppressors of cytokine signaling (SOCS) pathways to inhibit the host's ability to clear an infection (53). The effect of zebrafish infection with *Francisella* on the transcription of *socs1*, *socs3a*, and *socs3b* was therefore investigated. Both *socs3a* and *socs3b* showed a strong increase in transcription at all time points tested starting from the earliest one (6 hpi), when it was statistically significant only for *socs3b*, while transcription of *socs1* remained unaffected. A similar response was previously reported for *F. tularensis* infection in murine macrophages (53). There was less effect on other selected gene products, although complement component 3 showed a significant increase at 48 hpi. There was no difference in transcription of *ifng1-2* whatsoever. At 48 hpi there was a slight increase in *nos2a*, but the effect was small and variable between replicates.

(iii) *F. noatunensis* subsp. *orientalis*-mCh colocalization with zebrafish embryo phagocytes. In the early embryo the two prominent phagocytic cells, macrophages and neutrophils, can potentially play a role in bacterial uptake and GLS formation (54). To investigate which cells types were involved in these processes we took advantage of the two transgenic zebrafish lines with either macrophages [*Tg*(*mpeg1*:EGFP)*gl22*] (38) or neutrophils [*Tg*(*mpx*:EGFP)*i114*] expressing EGFP (39). *F. noatunensis* subsp. *orientalis*-mCh was injected into the duct of Cuvier of transgenic zebrafish embryos with fluorescently labeled macrophages. The transgenic zebrafish embryos were less robust than the wild type, with full mortality often observed 1 day earlier (data not shown). This might be related to the different genetic background of the zebrafish lines; however, it is unlikely to influence the early colocalization of *F. noatunensis* subsp. *orientalis*-mCh with immune cells to any significant extent. It was possible to detect single red fluorescent bacteria in the blood flow, followed by phagocytosis by macrophages within minutes after infection (see Video S1 in the supplemental material). Several hours later the majority of the

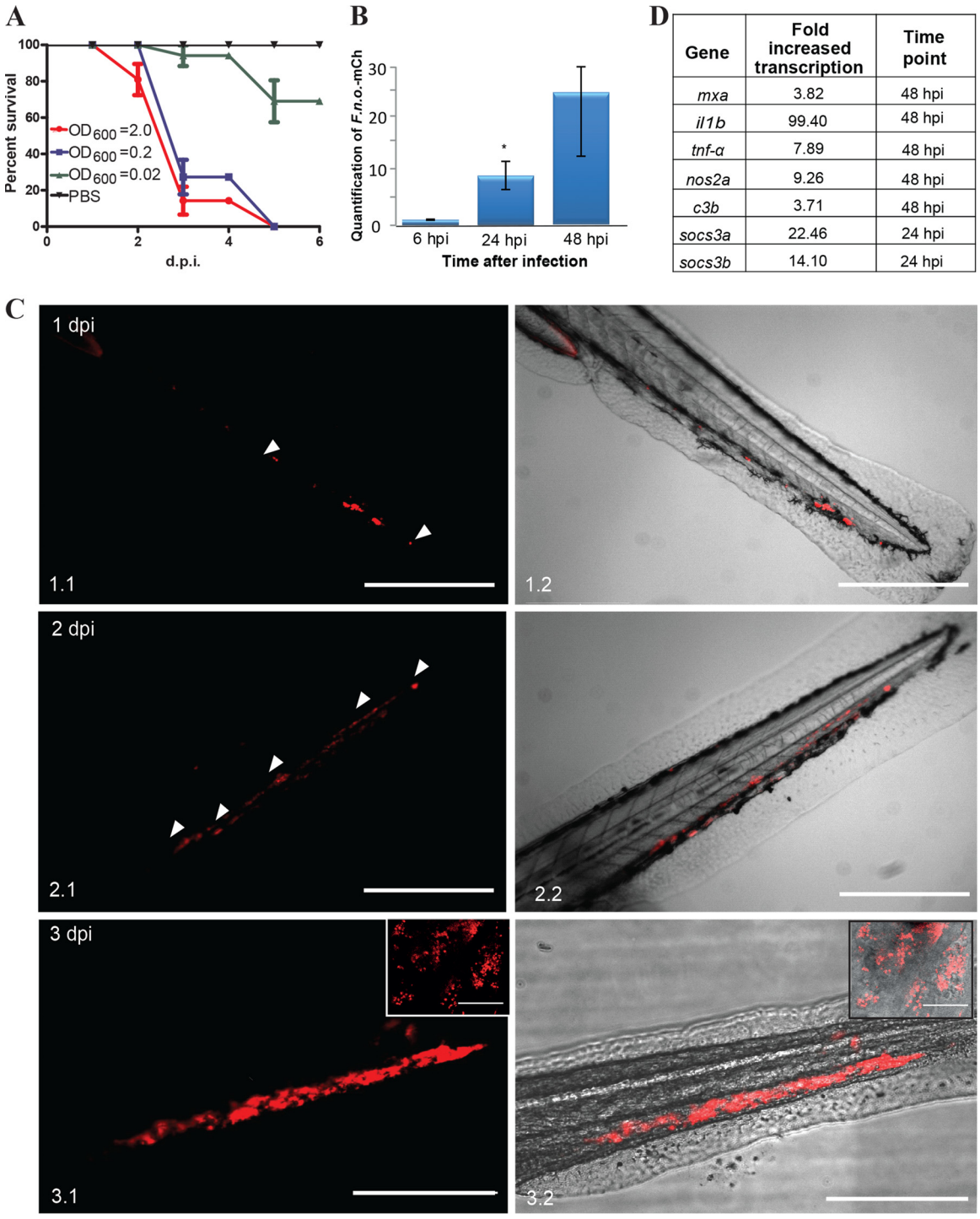

D

Gene	Fold increased transcription	Time point
mxa	3.82	48 hpi
il1b	99.40	48 hpi
tnf-α	7.89	48 hpi
nos2a	9.26	48 hpi
c3b	3.71	48 hpi
socs3a	22.46	24 hpi
socs3b	14.10	24 hpi

FIG 1 *F. noatunensis* subsp. *orientalis*-mCh infection of zebrafish embryos. (A) Kaplan-Meier representation of cumulative survival of zebrafish embryos infected with approximately 9×10^3 ($OD_{600} = 2$), 9×10^2 ($OD_{600} = 0.2$), and 9×10 ($OD_{600} = 0.02$) CFU *F. noatunensis* subsp. *orientalis*-mCh at 28°C. (B) Time-dependent growth of *F. noatunensis* subsp. *orientalis*-mCh in zebrafish embryos infected with 9×10^3 CFU. The asterisk indicates a statistically significant difference ($P < 0.05$). (C). Development of *F. noatunensis* subsp. *orientalis*-mCh granuloma-like structures in zebrafish embryos over time: 1 dpi (panels 1.1 and 1.2), 2 dpi (panels 2.1 and 2.2), and 3 dpi (panels 3.1 and 3.2). Insets show granuloma-like structures at higher magnification. (D) The most upregulated genes of zebrafish embryos infected with *F. noatunensis* subsp. *orientalis*-mCh. Scale bars, 200 μm (insets, 20 μm).

bacteria were phagocytized by macrophages (Fig. 2A, panels 1.1 and 1.2). Further imaging of *F. noatunensis* subsp. *orientalis*-mCh interaction with macrophages was complicated, as the fluorescent signal from the *Tg*(*mpeg1*:EGFP)*gl22* cells was lost at later time points. Transcription controlled by the *mpeg1* promoter has previously been shown to decrease in zebrafish when infected with *S.* Typhimurium (55). This could explain the lack of EGFP-expressing macrophages at 4 dpi in zebrafish infected with *F. noatunensis*

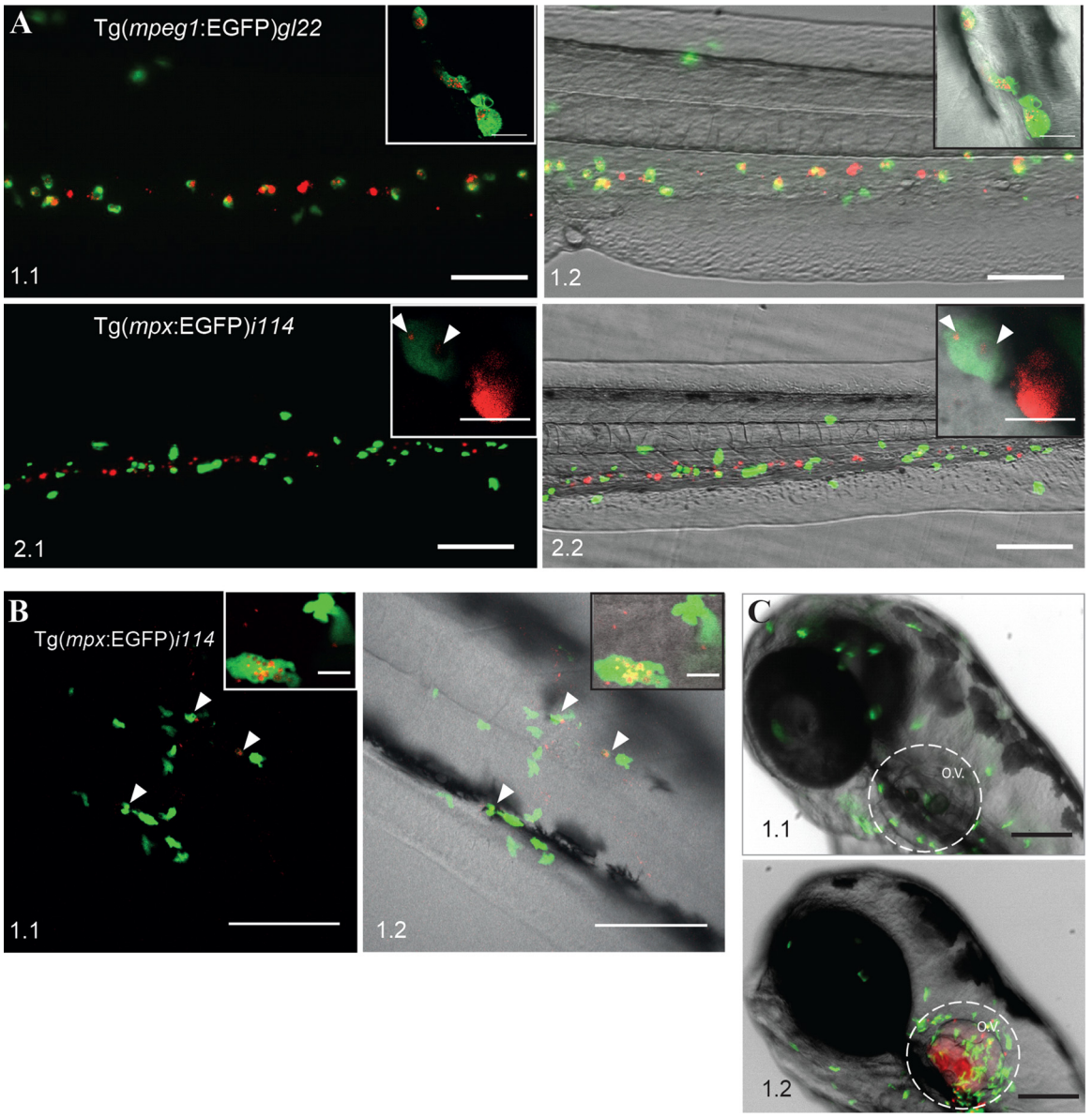

FIG 2 Interaction of *F. noatunensis* subsp. *orientalis*-mCh with innate immune cells of zebrafish embryos. (A) *F. noatunensis* subsp. *orientalis*-mCh colocalizes with EGFP-expressing macrophages in *Tg*(*mpeg1*:EGFP)*gl22* zebrafish embryos (panels 1.1 and 1.2; insets show single cells) at 3 hpi, whereas only a low degree of colocalization was observed with EGFP-expressing neutrophils in *Tg*(*mpx*:EGFP)*i114* zebrafish embryos (panels 2.1 and 2.2; inserts show a single neutrophil with few phagocytized bacteria and a highly loaded macrophage). (B) Neutrophils are attracted to infected tail muscle of *Tg*(*mpx*:EGFP)*i114* zebrafish embryos and efficiently phagocytize *F. noatunensis* subsp. *orientalis*-mCh (panels 1.1 and 1.2; insets show single cells) at 3 hpi. (C) Neutrophils are attracted to *F. noatunensis* subsp. *orientalis*-mCh infected otic vesicle of *Tg*(*mpx*:EGFP)*i114* zebrafish embryos (panel 1.2), in contrast to the control zebrafish injected with PBS at 3 hpi (panel 1.1). Scale bars, 100 μm (A and C) and 50 μm (B) (insets, 20 μm [A, panels 1.1 and 1.2] and 10 μm [A, panels 2.1 and 2.2]).

subsp. *orientalis*-mCh despite the presence of bacterial aggregates in the tissue, presumably representing intracellular *F. noatunensis* subsp. *orientalis*-mCh in macrophages. In contrast to the data obtained for macrophages, when the zebrafish strain with EGFP-expressing neutrophils was injected intravascularly (duct of Cuvier) with *F. noatunensis* subsp. *orientalis*-mCh, the amount of bacteria colocalizing with neutrophils was much lower (Fig. 2A, panels 2.1 and 2.2). High-resolution confocal microscopy revealed that even though neutrophils were able to take up *F. noatunensis* subsp. *orientalis*-mCh, they were less efficient than macrophages (Fig. 2A, panels 2.1 and 2.2, insets). Nevertheless, these observations showed that both lineages of zebrafish phagocytes were able to take up the bacteria.

It has been shown that zebrafish embryonic neutrophils prefer a solid surface for efficient phagocytosis of *E. coli* (54), and we could substantiate this finding using fluorescent *E. coli*. *Tg*(*mpx*:EGFP)*i114* zebrafish embryos were then injected with *F. noatunensis* subsp. *orientalis*-mCh into the tail muscle at 3 days postfertilization (dpf) to investigate whether *Francisella* spp. can be phagocytized by neutrophils more efficiently than after intravenous injection. Tail muscle infection was followed by several hours of *in vivo* high-resolution confocal microscopy imaging. We

observed a strong attraction of neutrophils to the injection site, consistent with an inflammatory response (Fig. 2B), and indeed the activated neutrophils had a higher bacterial burden than was the case when the fish were infected via the circulatory system (Fig. 2B). The ability of *F. noatunensis* subsp. *orientalis*-mCh to attract neutrophils was even more evident when *F. noatunensis* subsp. *orientalis*-mCh was injected into the otic vesicle (ear), which prior to the infection was devoid of neutrophils (Fig. 2C). A strong neutrophil attraction to the vicinity of the otic vesicle was observed at 3 hpi (Fig. 2C).

In summary, *F. noatunensis* subsp. *orientalis*-mCh was capable of entering both lineages of zebrafish phagocytes. The macrophages were clearly the main phagocytes for taking up the bacteria. Nevertheless neutrophils were also rapidly attracted to the bacteria but were able to phagocytize them efficiently only when *F. noatunensis* subsp. *orientalis*-mCh were present on a surface (muscle tissue).

Model 2, infection of zebrafish with *F. noatunensis* subsp. *noatunensis* at 22°C: *F. noatunensis* subsp. *noatunensis* infection of zebrafish embryos causes chronic disease. *F. noatunensis* subsp. *noatunensis* has an optimal growth temperature of 20 to 22°C. Therefore, the infected embryos were kept at 22°C after infection and at 28°C prior to it. In striking contrast to infections with *F. noatunensis* subsp. *orientalis*-mCh, the *F. noatunensis* subsp. *noatunensis*-infected zebrafish embryos showed no significant mortality regardless of the bacterial load used for infection (OD_{600} of 0.2 or 2.0) (Fig. 3A). *F. noatunensis* subsp. *noatunensis*-GFP was detected in infected embryos by RT-qPCR at 6 hpi (Fig. 3B), and although no significant bacterial growth was observed by 24 hpi, there was an approximately 13-fold increase in the amount of bacteria in the fish by 7 dpi, yielding an estimated doubling time of 43 h. The lower growth rate *in vivo* of *F. noatunensis* subsp. *noatunensis* compared to *F. noatunensis* subsp. *orientalis* likely reflects the lower *in vitro* growth rate of this strain. This absence of mortality is similar to the situation in the natural host, the Atlantic cod, when experimentally challenged with *F. noatunensis* subsp. *noatunensis*. In this host, even when injecting high doses of bacteria, there is often a lack of mortality although formation of granulomas is visible by the naked eye (5, 29, 56).

(i) Imaging of GLS development in *F. noatunensis* subsp. *noatunensis*-GFP-infected zebrafish embryos. It was possible to detect GLS formation within 3 days postinfection of embryos with *F. noatunensis* subsp. *noatunensis*-GFP via the intravenous route. The GLS were distributed throughout the fish (Fig. 3C). The size, number, and fluorescent intensity of GLS increased with time, indicating growth of the bacteria in infected embryos. The development of the GLS (Fig. 3C) resembled that seen with *F. noatunensis* subsp. *orientalis*-mCh infection; however, consistent with the lower temperature used for *F. noatunensis* subsp. *noatunensis*, the formation of GLS was observed 1 to 2 days later than in the case with *F. noatunensis* subsp. *orientalis*-mCh infection.

When embryos were kept at their optimal growth temperature of 28°C, it was not possible to detect significant amounts of *F. noatunensis* subsp. *noatunensis*-GFP by fluorescent imaging after intravascular injections, suggesting that this temperature is not compatible with bacterial proliferation. This is in agreement with the *in vitro* growth characteristics of *F. noatunensis* subsp. *noatunensis* (57).

(ii) Immune response of zebrafish embryos infected with *F. noatunensis* subsp. *noatunensis*-GFP. The immune response of zebrafish embryos to *F. noatunensis* subsp. *noatunensis*-GFP infection was dominated by the same pattern as the immune response to *F. noatunensis* subsp. *orientalis*-mCh, although it was somewhat delayed and reduced (Fig. 3D; see Fig. S3 in the supplemental material). The transcription levels of *tnfa* increased by 15-fold, those of *il10* increased by 4-fold, those of complement factor increased by 3- to 6-fold, those of *ifng1-2* increased by 5.1-fold, and those of *il1b* reached a 30-fold increase on 7 dpi and were slightly elevated at 24 hpi (approximately a 2-fold increase). With regard to the *socs* genes, no change was detected for *socs1*; however, statistically significant differences were detected for *socs3a* at 24 hpi and *socs3b* at 7 dpi (2.1- and 0.85-fold increases, respectively). The slight elevation of *socs3* was markedly reduced compared to the increase observed in zebrafish embryos infected with *F. noatunensis* subsp. *orientalis*-mCh, probably reflecting a lower bacterial burden and/or a temperature dependency in the host response.

(iii) Interaction of *F. noatunensis* subsp. *noatunensis*-mCh with zebrafish embryo immune cells. To allow for colocalization studies of *F. noatunensis* subsp. *noatunensis* with transgenic zebrafish strains expressing EGFP-labeled immune cells, wild-type *F. noatunensis* subsp. *noatunensis* was transformed with the pKK289Km plasmid containing the *mCherry* gene in exchange for *gfp*. The zebrafish embryos infected with *F. noatunensis* subsp. *noatunensis*-mCh showed the same survival curves as the wild-type fish (data not shown). Colocalization of a majority of the bacteria and macrophages was observed as early as 3 hpi (Fig. 4A) and lasted for at least another 5 days. Clusters of bacteria not colocalized with EGFP-expressing macrophages were also visible at 4 dpi (data not shown). This observation suggests that these bacteria were able to kill the macrophages and reside free in the tissue or, more likely, represent intracellular bacteria in macrophages which have lost their fluorescence as a result of downregulation of EGFP expression at later time points of infection, as discussed above. Similar to the case for *F. noatunensis* subsp. *orientalis*-mCh infection, the amount of bacteria colocalizing with neutrophils was much less than that for macrophages (Fig. 4A), although small amounts of *F. noatunensis* subsp. *noatunensis*-mCh could be detected inside neutrophils after intravascular injections when observed by confocal microscopy (Fig. 4A, panels 2.1 and 2.2, insets). Therefore, macrophages are the main cells responsible for phagocytosis of intravascularly injected *F. noatunensis* subsp. *noatunensis*-mCh as well. Infection of *Tg*(*mpx*:EGFP)*i114* zebrafish embryos with *F. noatunensis* subsp. *noatunensis*-mCh was also performed by injections into the tail muscle (Fig. 4B) and otic vesicle (Fig. 4C). Imaging of the fish at 3 hpi revealed that neutrophils were strongly attracted to the sites of injections. Confocal microscopy identified small numbers of intracellular bacteria in neutrophils when *F. noatunensis* subsp. *noatunensis*-mCh was injected into tissue, verifying that *F. noatunensis* subsp. *noatunensis* also is able to infect this phagocytic cell (Fig. 4B, panels 1.1. and 1.2, insets).

Model 3, infection of zebrafish embryos with *F. tularensis* subsp. *novicida* at 32°C: *F. tularensis* subsp. *novicida* causes 60% mortality in zebrafish embryos. When injected into the duct of Cuvier, *F. tularensis* subsp. *novicida*-GFP was capable of causing mortality of embryos kept at both the optimal temperature for the embryos (28°C) and an elevated temperature more adapted to bacterial growth (32°C). *F. tularensis* subsp. *novicida*-GFP infection developed at a lower rate than *F. noatunensis* subsp. *orientalis*-mCh infection. Cumulative mortality after 6 days for the embryos

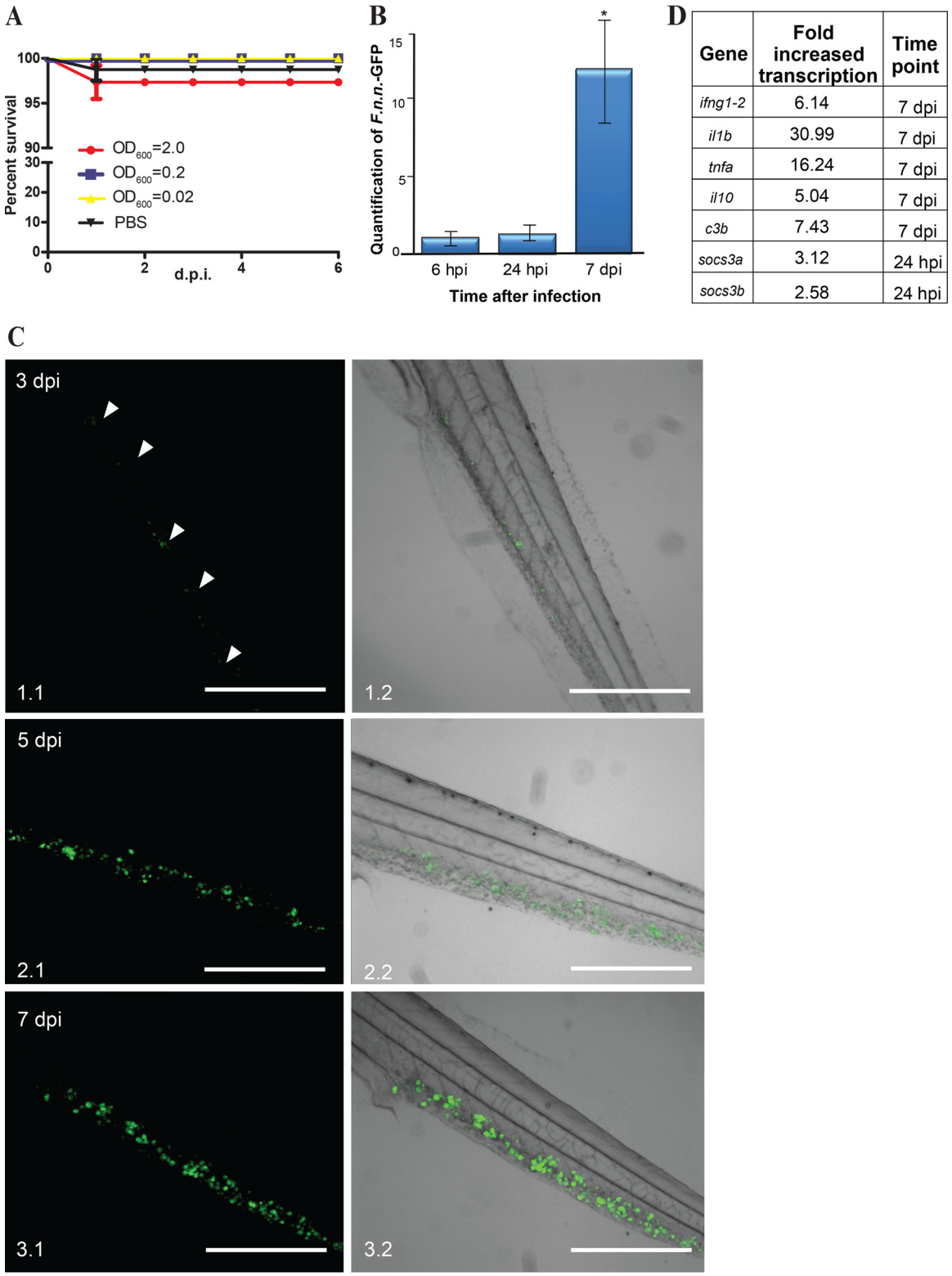

D

Gene	Fold increased transcription	Time point
ifng1-2	6.14	7 dpi
il1b	30.99	7 dpi
tnfa	16.24	7 dpi
il10	5.04	7 dpi
c3b	7.43	7 dpi
socs3a	3.12	24 hpi
socs3b	2.58	24 hpi

FIG 3 *F. noatunensis* subsp. *noatunensis*-GFP infection of zebrafish embryos. (A) Kaplan-Meier representation of cumulative survival of zebrafish embryos infected with approximately 9×10^3 ($OD_{600} = 2$), 9×10^2 ($OD_{600} = 0.2$), and 9×10 ($OD_{600} = 0.02$) CFU of *F. noatunensis* subsp. *noatunensis*-GFP at 22°C. (B) Time-dependent growth of *F. noatunensis* subsp. *noatunensis*-GFP in zebrafish embryos infected with 9×10^3 CFU. The asterisk indicates a statistically significant difference ($P < 0.05$). (C) Development of *F. noatunensis* subsp. *noatunensis*-GFP granuloma-like structures in zebrafish embryos over time: 3 dpi (panels 1.1 and 1.2), 5 dpi (panels 2.1 and 2.2), and 7 dpi (panels 3.1 and 3.2). (D) The most upregulated genes of zebrafish embryos infected with *F. noatunensis* subsp. *noatunensis*-GFP. Scale bars, 200 μm.

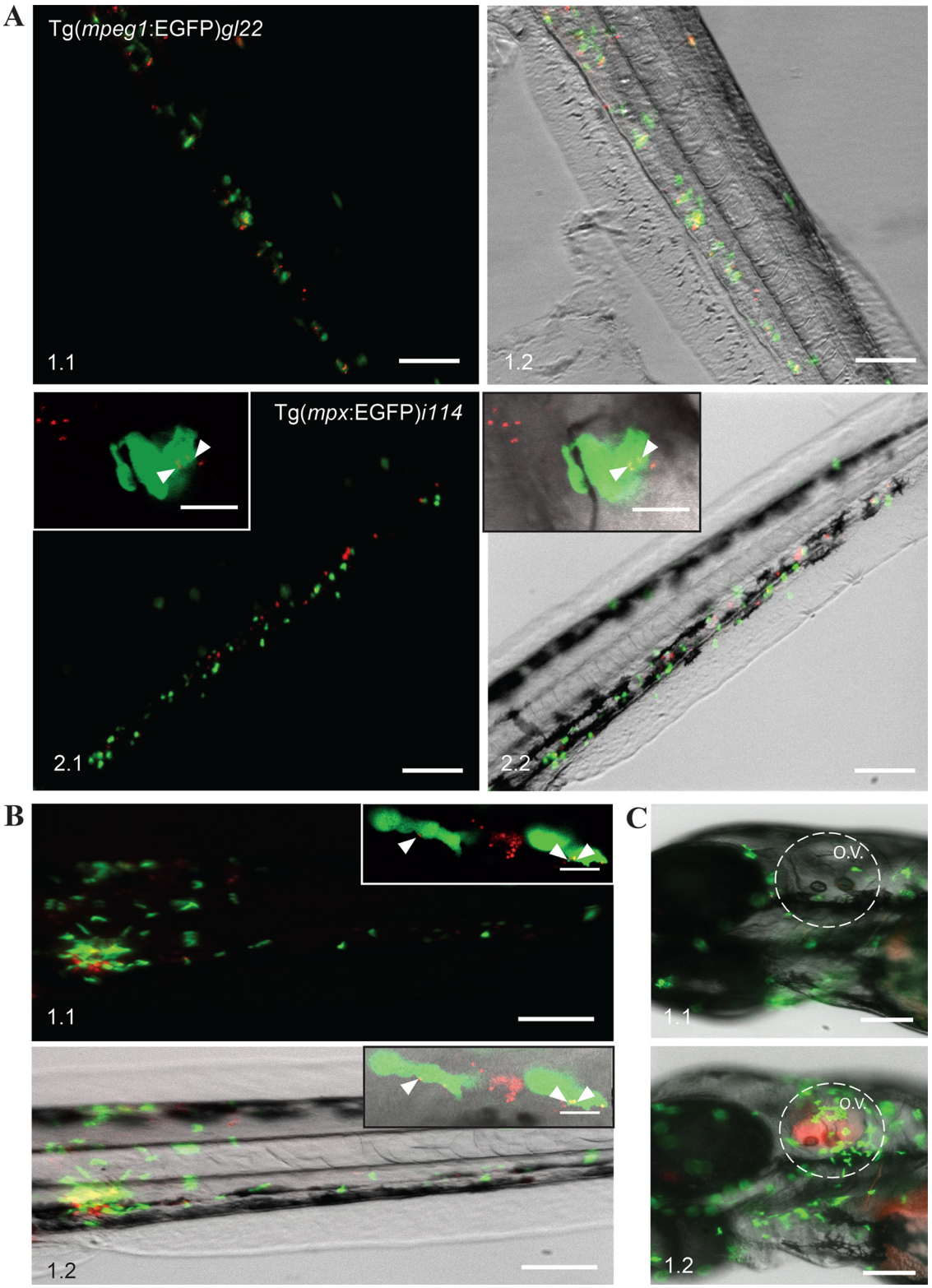

FIG 4 Interaction of *F. noatunensis* subsp. *noatunensis*-mCh with innate immune cells. (A) Colocalization of *F. noatunensis* subsp. *noatunensis*-mCh and macrophages in *Tg*(*mpeg1*:EGFP)*gl22* zebrafish embryos (panels 1.1 and 1.2) and no or little colocalization between *F. noatunensis* subsp. *noatunensis*-mCh and neutrophils in the *Tg*(*mpx*:EGFP)*i114* zebrafish line at 3 hpi (panels 2.1 and 2.2; insets show neutrophils with few phagocytized bacteria). (B) Injection of *Tg*(*mpx*:EGFP)*i114* zebrafish embryos with *F. noatunensis* subsp. *noatunensis*-mCh suspension into the tail muscle demonstrates attraction of neutrophils to the bacteria followed by phagocytosis at 3 hpi (panels 1.1 and 1.2). Insets show slightly loaded neutrophils and a macrophage with a high red fluorescent bacterial burden. (C) The otic vesicle of *Tg*(*mpx*:EGFP)*i114* zebrafish embryos injected with PBS (panel 1.1) excludes neutrophils, while they are attracted in the case of *F. noatunensis* subsp. *noatunensis*-mCh infection (panel 1.2). Scale bars, 100 μm (insets, 10 μm).

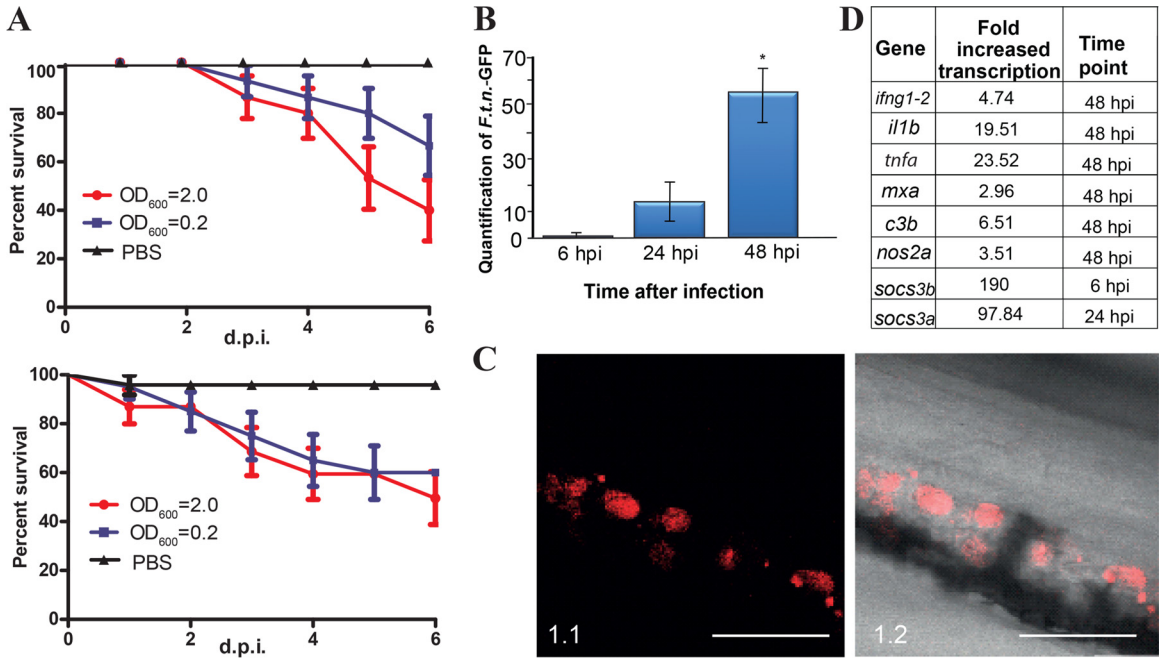

D

Gene	Fold increased transcription	Time point
ifng1-2	4.74	48 hpi
il1b	19.51	48 hpi
tnfa	23.52	48 hpi
mxa	2.96	48 hpi
c3b	6.51	48 hpi
nos2a	3.51	48 hpi
socs3b	190	6 hpi
socs3a	97.84	24 hpi

FIG 5 *F. tularensis* subsp. *novicida*-GFP infection of zebrafish embryos. (A) Kaplan-Meier representation of cumulative survival of zebrafish embryos infected with approximately 3×10^4 (OD_{600} = 2.0) and 3×10^3 (OD_{600} = 0.2) CFU of *F. tularensis* subsp. *novicida*-GFP and kept at 28°C (upper graph) or 32°C (lower graph). (B) Time-dependent growth of *F. tularensis* subsp. *novicida*-GFP in zebrafish embryos infected with 3×10^4 CFU. The asterisk indicates a statistically significant difference ($P < 0.05$). (C). Granuloma-like structures in zebrafish infected with *F. tularensis* subsp. *novicida*-mCh at 4 dpi. (D) The most upregulated genes of zebrafish embryos infected with *F. tularensis* subsp. *novicida*-GFP. Scale bar, 100 μm.

infected with *F. tularensis* subsp. *novicida*-GFP at an OD_{600} of 2.0 reached 60% and 50% at 28°C and 32°C, respectively (Fig. 5A). The onset of mortality occurred earlier at 32°C even though the cumulative mortality was almost equal at 32°C and 28°C. Zebrafish embryos tolerated the elevated temperature well, showing no abnormalities in behavior or development. Taking these data into consideration, the remaining experiments were carried out at 32°C to approach the normal growth conditions of *F. tularensis* subsp. *novicida*. *F. tularensis* subsp. *novicida* grows faster than the *Francisella* fish pathogens *in vitro*, which was also reflected in the bacterial growth rate in infected fish at 32°C as determined by RT-qPCR. *F. tularensis* subsp. *novicida*-GFP increased by 16-fold from 6 hpi to 24 hpi and by more than 55-fold by 48 hpi (Fig. 5B), yielding an estimated doubling time of 7 h.

(i) Imaging of zebrafish embryos infected with *F. tularensis* subsp. *novicida*-GFP. A peculiarity of *F. tularensis* subsp. *novicida*-GFP infection led to moderate GLS formation compared to that with *F. noatunensis* infections. A common observation was several small bacterial aggregations rather than the larger aggregates seen with the two other strains of *Francisella* used in this study (Fig. 5C). Even though zebrafish embryos heavily loaded with granulomas were observed in the infected groups, those were not numerous (data not shown). The factors responsible for the observed differences in disease development remain to be investigated even though this can arguably be explained by the fact that the infection studies were performed at a temperature 5°C lower than optimal for growth of *F. tularensis* subsp. *novicida*.

(ii) Immune response of zebrafish embryos infected with *F. tularensis* subsp. *novicida*-GFP. The zebrafish embryo host immune response to *F. tularensis* subsp. *novicida*-GFP infection, as evaluated by RT-qPCR, revealed increased transcription of key immune molecules, dominated by *il1b* and *tnfa*, starting as early as 6 hpi (Fig. 5D; see Fig. S4 in the supplemental material). Other immune-related genes showed less response, though *c3b*, *mxa*, and *il12a* also showed statistically significantly increased transcription. Additionally, *nos2a* was increased at 48 hpi, although only by a factor of 2.5. Interestingly, the *socs3* genes exhibited a fast and strong response, especially *socs3b* (189-fold increase at 6 hpi and 94-fold increase at 24 hpi). The *socs3a* gene responded slower, with a 4-fold increase (not statistically significant) at 6 hpi and a 96-fold increase at 24 hpi. No transcriptional differences were observed for *socs1*, except for a slight elevation (0.75-fold) at 48 hpi.

(iii) Interaction of *F. tularensis* subsp. *novicida* with host immune cells. Infection of the previously mentioned transgenic zebrafish embryos with *F. tularensis* subsp. *novicida*-mCh resulted in an outcome similar to those for *F. noatunensis* subsp. *orientalis*-mCh and *F. noatunensis* subsp. *noatunensis*-mCh. Intravascularly injected *F. tularensis* subsp. *novicida*-mCh preferably entered macrophages (Fig. 6A). Neutrophils were strongly attracted to the sites of bacterial location (Fig. 6B and C), though they were even less efficient in phagocytizing *F. tularensis* subsp. *novicida*-mCh (Fig. 6A; see Video S2 in the supplemental material) than in the case of *F. noatunensis* subsp. *orientalis*-mCh and *F. noatunensis* subsp. *noatunensis*-mCh when the bacteria were injected into circulation. *F. tularensis* subsp. *novicida*-mCh was taken up by neutrophils in the tail muscle infection (Fig. 6B; see Video S3 in the supplemental material), as seen for the two *F. noatunensis* subspecies. Interestingly, *F. tularensis* subsp. *novicida*-mCh was detected in neutrophils also at later stages of the infection (4 dpi), when GLS are formed (see Video S4 in the supplemental material), though the majority of the bacteria remained colocalized with

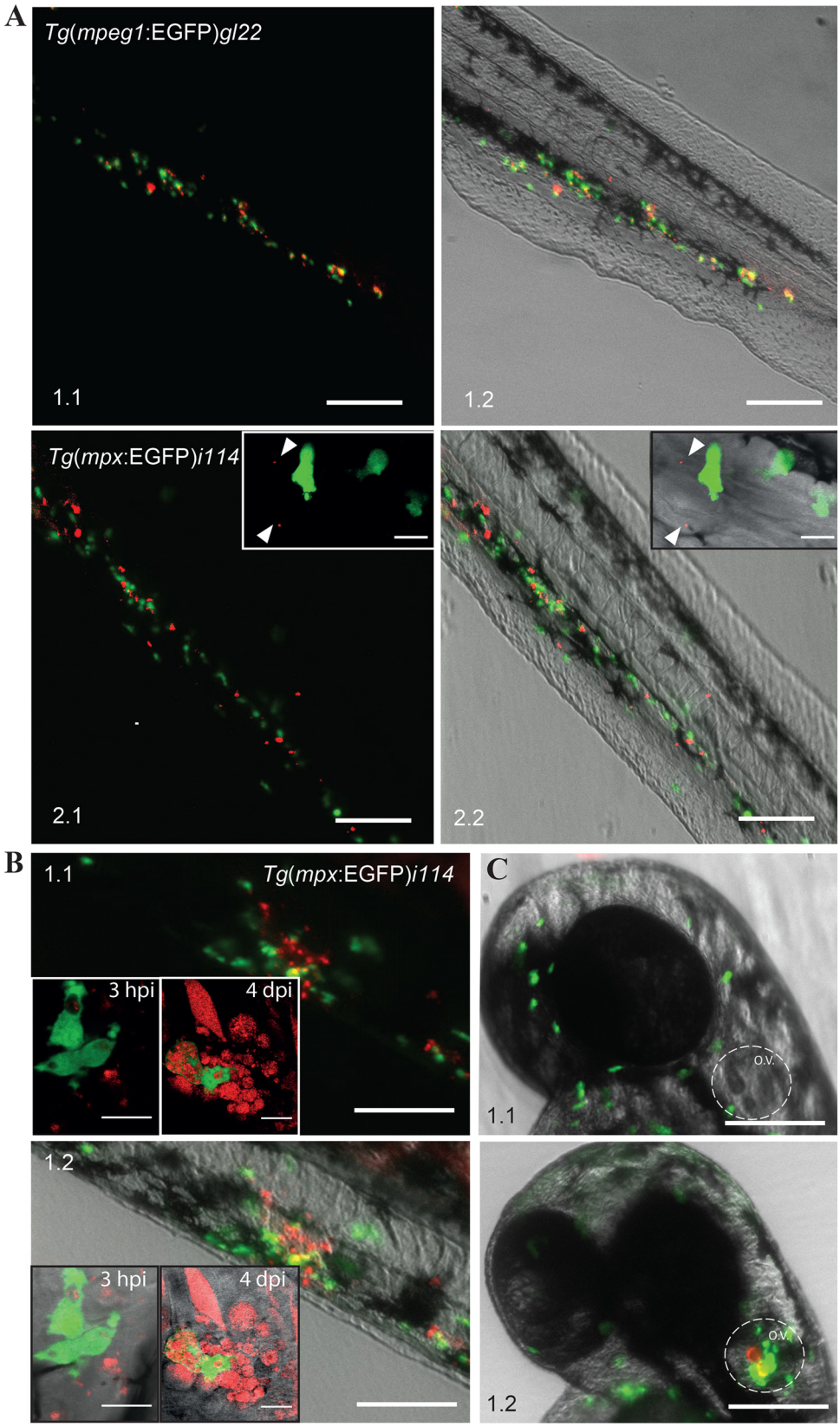

FIG 6 Interaction of *F. tularensis* subsp. *novicida*-mCh with innate immune cells. (A) EGFP-expressing macrophages in *Tg*(*mpeg1*:EGFP)*gl22* zebrafish embryos show a high degree of colocalization with *F. tularensis* subsp. *novicida*-mCh (panels 1.1 and 1.2), but EGFP-expressing neutrophils in *Tg*(*mpx*:EGFP)*i114* zebrafish embryos and *F. tularensis* subsp. *novicida*-mCh are not often found to be colocalized (panels 2.1 and 2.2). Insets show single neutrophils at 3 hpi. (B) *Tg*(*mpx*:EGFP)*i114* zebrafish embryos injected with *F. tularensis* subsp. *novicida*-mCh suspension into tail muscle. Neutrophils are attracted to the site of injection and are able to phagocytize the bacteria at 3 hpi. (C) Neutrophils are attracted to *F. tularensis* subsp. *novicida*-mCh-infected otic vesicle of *Tg*(*mpx*:EGFP)*i114* zebrafish embryos (panel 1.2) but not in the case of PBS injection (panel 1.1). Scale bars, 100 μm (insets, 10 μm).

macrophages (Fig. 6B, panels 1.1 and 1.2, insets). This suggests that *F. tularensis* subsp. *novicida*-mCh is able to survive in neutrophils after phagocytosis.

DISCUSSION

Due to the highly transparent embryonic stage, the zebrafish is increasingly used as a robust model system for the analysis of various bacterial infections (31, 54, 58). Our present study increases the value of this model by showing that zebrafish embryos can be adapted to significantly different temperatures to monitor infections with three different strains of *Francisella*. Two of these strains are important pathogens of aquaculture fish. *F. noatunensis* subsp. *noatunensis* is a pathogen of "cold-water" fish such as Atlantic cod and Atlantic salmon, and it could infect but not kill the embryos at 22°C. *F. noatunensis* subsp. *orientalis*, which infects "warm-water" commercial fish such as tilapia and has the same optimal growth temperature as zebrafish (28°C), caused rapidly developing disease and lethality in zebrafish embryos. For the third strain, *F. tularensis* subsp. *novicida*, a mouse pathogen that is widely used as a model for the human pathogen *F. tularensis* subsp. *tularensis*, the embryos were kept at 32°C in a compromise between optimal growth conditions for the bacteria and maintaining good health of the zebrafish embryos. Such a compromise could be the reason for a relatively mild infection with intermediate mortality, in spite of strong bacterial growth.

Although the preferred growth temperature of the zebrafish is 28°C, the embryos adapted well to both increased and decreased temperatures, in agreement with earlier studies focusing on viral infections of embryos at 24°C and for short periods of time at 15°C (49, 59). No abnormalities were evident in the appearance, behavior, or mortality profiles of noninfected embryos at the different temperatures. At all temperatures tested, the three bacterial strains could successfully infect the fish regardless the route of infection (circulatory system, tail muscle, or otic vesicle). The qPCR analysis showed that all three bacterial strains were able to multiply in zebrafish embryos infected via the intravascular route. The generation intervals for the different *Francisella* strains reflected their *in vitro* growth characteristics. The fastest-growing *F. tularensis* subsp. *novicida* has a generation interval of about 5 h in broth (60), which is only slightly less than the estimated 7 h observed *in vivo* in this study. The shorter doubling time in zebrafish of *F. noatunensis* subsp. *orientalis* (9 h) than of *F. noatunensis* subsp. *noatunensis* (43 h) is in agreement with the *in vitro* growth rates of these strains (37) also estimated by CFU counts (unpublished data).

The responses of the embryos to the different *Francisella* species were similar, based on a number of criteria. First, there was significant replication of all three bacterial strains as determined by RT-qPCR, despite a pronounced response by the fish immune system. Second, mCherry-labeled bacteria of all three species interacted similarly with zebrafish immune cells. These data were revealed by taking advantage of the availability and ease of imaging of different marker cell types in transgenic zebrafish lines. The EGFP-fluorescing macrophage transgenic fish line *Tg*(*mpeg1*:EGFP)*gl22* has been previously used in other studies for determining the association of pathogens with these cells (see, e.g., reference 61). Here, the use of this transgenic fish (38) clearly demonstrated that the macrophage is the main *Francisella*-phagocytizing cell type, which is in agreement with earlier studies with mouse and human macrophages (62, 63). Imaging of the formed GLS showed that macrophages were the major site of *Francisella* residence, and even though the bacteria persisted in neutrophils, the amount was still limited at 4 dpi. Since the half-life of zebrafish neutrophils is 120 h (64), we observed the same cells over a few days. Therefore, it can be argued that *Francisella* does not multiply in neutrophils and that the main site of replication is probably within macrophages.

Using the EGFP-expressing neutrophil line *Tg*(*mpx*:EGFP)*i114* (39) allowed observation of strong neutrophil attraction to the sites of bacterial location, though in comparison to macrophages, these cells were less efficient at phagocytosis of *Francisella* spp., particularly from the circulatory system. Previously, Colucci-Guyon et al. (54) reported that zebrafish neutrophils required a surface for efficient phagocytosis of nonpathogenic *E. coli*. We also observed efficient neutrophil uptake of *E. coli* pmCherry injected into tissue, and we extended the observation by showing that this striking behavior is also valid for pathogenic *Francisella* strains (Fig. 2A and B, 4A and B, and 6A and B). In the case of intravenous infections, neutrophils showed only modest phagocytic activity toward *F. noatunensis* subsp. *orientalis* and *F. noatunensis* subsp. *noatunensis* and were not found to colocalize at all with *F. tularensis* subsp. *novicida* Even though neutrophils appeared to be more successful in taking up *Francisella* subsp. from the tail muscle substrate, they were still less efficient in overall phagocytosis than macrophages. Our findings are consistent with existing reports of bacterial interaction with immune cells in their natural hosts. For example, previous studies of *F. noatunensis* subsp. *noatunensis* in Atlantic cod showed bacteria in the close proximity of neutrophils but never or rarely inside them (22, 56). *F. tularensis* subsp. *novicida* has been demonstrated to be efficiently taken up by neutrophils in a mouse pulmonary infection model (63), similar to the results for *F. tularensis* subsp. *novicida* injected into muscle tissue observed in this study. Regardless of the potential efficiency of phagocytosis, the results show that all three strains of *Francisella* investigated in this study were taken up by both lineages of zebrafish phagocytes. The efficiency of zebrafish neutrophils in phagocytizing bacteria in blood is likely to be dependent on the specific bacterial species, as intravascularly injected *Pseudomonas aeruginosa* is efficiently taken up and killed by zebrafish neutrophils (65).

The third criterion that was similar for the three bacterial infections was the fact that the infected macrophages could assemble into what we operationally define as granuloma-like structures (GLS). Differences were noted in the strength of the granulomatous response, with the largest GLS seen with *F. noatunensis* subsp. *orientalis* at 28°C and the least developed ones seen with *F. tularensis* subsp. *novicida* at 32°C. We hypothesize that the studied *Francisella* species have different potentials for causing GLS formation in zebrafish, which might also be influenced by the differences in temperature. The fourth criterion of similarity came from the analysis of the innate immune response of the embryos to the three bacterial strains, as similar patterns of gene transcription were seen. Increased mRNAs levels for *il1b*, *tnfa*, and *socs3b* in all three strains were observed, with less but still significantly increased transcription of *c3b*, *il10*, *il12a*, and *ifng1-2* for some strains. The fifth criterion indicative of a successful infection by two of the three pathogens was their ability to kill all of *F. noatunensis* subsp. *orientalis*-infected, and a significant fraction of *F. tularensis* subsp. *novicida*-infected, embryos. An exception was seen with *F. noatunensis* subsp. *noatunensis*, which failed to kill any embryos in the time frame of the experiment at 22°C. This bacterium induced a chronic rather than a lethal infection. Inter-

estingly, *F. noatunensis* subsp. *noatunensis* causes similar chronic infections in its natural host, the Atlantic cod (4, 29, 55), highlighting the strong potential of the zebrafish model. Another significant difference in the immune response of *F. noatunensis* subsp. *noatunensis* that was not seen with the other two bacteria was an induction of the anti-inflammatory cytokine IL-10; this might contribute to the absence of lethality with *F. noatunensis* subsp. *noatunensis*, as well as the lower growth rate of *F. noatunensis* subsp. *noatunensis* compared to the two other strains in infected fish. A lack of IL-10 production in systemic infections can result in higher levels of proinflammatory cytokines, more tissue damage, and earlier death, while excessive production of IL-10 can cause decreased ability to clear pathogens, resulting in chronic or lethal infections (66).

An earlier study by Vojtech et al. (36) showed that adult zebrafish at 28°C could be infected with a strain of *F. noatunensis* subsp. *orientalis* that induced impressive early GLS formation, as seen by histological examination. While the adult fish has both the innate and adaptive immune systems operating, the embryos have only innate immunity. Thus, it is notable that two of the immune gene products that were strongly upregulated in the analysis of adult fish, namely, *il1b* and *tnfa*, were also prominently elevated in our infected zebrafish embryos. One clear difference was that whereas the transcription of *ifng1-2* was increased in adult fish, we saw no significant elevation in the embryos in response to infection with *F. noatunensis* subsp. *orientalis* (although it was upregulated with *F. noatunensis* subsp. *noatunensis* and *F. tularensis* subsp. *novicida*). The increased transcription of *il1b*, *il10*, and *ifng1-2* at 7 dpi for *F. noatunensis* subsp. *noatunensis* also resembles the gene transcription results seen in Atlantic cod (29) and primary macrophages isolated from Atlantic cod (21). This argues that immune responses initiated upon recognition of *Francisella* spp. are conserved between different fish species and *Francisella* strains. Obviously, the additional activity of the adaptive immune system is crucial for full defense against *Francisella*, as Vojtech and colleagues found that 10^6 CFU of *F. noatunensis* subsp. *orientalis* was needed to kill 100% of adult fish (36), whereas only 9×10^2 CFU led to the same result for zebrafish embryos.

The question of how *Francisella* spp. are able to persist in infected macrophages, despite their potential to kill and degrade phagocytized pathogens, is crucial for understanding the pathogenesis of *Francisella* infections. It has previously been shown for *Francisella* that TNF-α and IFN-γ are responsible for inducing inhibition of bacterial growth and activation of bacterial killing by macrophages and that this effect is directly related to increased production of nitric oxide (NO) (67). NO is generated in macrophages by the inducible NO synthase (iNOS), the transcription of which is induced through the JAK-STAT signaling pathway by IFN-γ and through NF-κB activation by TNF-α and IFN-γ (68). In spite of our observations of increased transcription of these genes, neither we nor Vojtech et al. (36) could observe strong increases in other expected downstream effector systems, such as iNOS. This bacterium-induced inhibition is thought to be mediated by active inhibition by a bacterial heat-stable factor that has been shown to work in mammals by inhibiting STAT-dependent signaling by increased transcription of *socs3* (53). The SOCS proteins have been identified in many fish species (69), including zebrafish, and increased transcription of *socs3* was observed in response to infection of zebrafish embryos with all three *Francisella* strains. This argues that the active suppression of the host immune response in infection by *Francisella* spp. is an ancient mechanism that is conserved between different *Francisella* species and between mammals and fish. *Mycobacterium marinum* and *S.* Typhimurium have previously been reported to induce *socs3* in zebrafish (55, 70), opening up the possibility that this is a common pathway used by facultative intracellular bacteria to inhibit activation of zebrafish macrophages.

In conclusion, we have expanded the strength of zebrafish embryos as a powerful and robust model for studying bacterial pathogenesis, adding three *Francisella* subspecies to the list of microorganisms to which the embryos are susceptible. This opens up new possibilities for studying *Francisella* pathogenesis due to the capability for *in vivo* imaging of early events that happen right after infection. Zebrafish embryos appeared to be a reliable model at three different temperatures without apparent adverse effects on their health. We clearly showed the major role of macrophages in the phagocytosis of invading *Francisella* cells. Neutrophils were capable of quickly responding to the infection by migrating to the bacterial locations, though they had a variable degree of success in phagocytizing bacteria, depending on the route of infection. Our data also demonstrate that the host response to *Francisella* infections is similar for different species. Conclusively, the data obtained in this study lay a solid background for further investigation of the infections caused by different *Francisella* species.

ACKNOWLEDGMENTS

We greatly appreciate the support of Jan-Roger Torp Sørby and Peter Alestrom in setting up the zebrafish facility in the Institute of Biological Sciences and the help of Jan-Roger Torp Sørby and Ana Carolina Sulen Tavara in maintaining our fish stocks. We thank Stephen Renshaw and Graham Leischke for permission to use the *Tg*(*mpx1*:EGFP)*i114* and *Tg*(*mpeg1*:EGFP)*gl22* transgenic strains, respectively, and Annemarie Meijer for sending us these strains. The pKK289Km/*gfp* plasmid was a kind gift from Emelie N. Salomonsson, and the *F. tularensis* subsp. *novicida* wt strain was a kind gift from Tina Guina and Åke Forsberg. The *F. noatunensis* subsp. *orientalis* wt strain was a kind gift from Duncan J. Colquhoun. We also thank Tor Gjøen for lending us the primers to carry out some of the zebrafish immune response studies.

This work was supported by funds from the Norwegian School of Veterinary Sciences (E.B.), the University of Oslo (L.S.U. and E.O.L), and the Research Council of Norway.

E.B. planned and performed some of the experiments and was involved in writing the paper. L.S.U. planned and performed some of the experiments and was involved in writing the paper. E.O.L. planned and performed some of the experiments. A.-L.R. performed some of the experiments. G.G.'s group set up the zebrafish facility and contributed to planning the experiments and writing the paper. H.C.W-L. performed some of the experiments and contributed to the design of the experiments and writing the paper.

REFERENCES

1. **Ellis J, Oyston PC, Green M, Titball RW.** 2002. Tularemia. Clin. Microbiol. Rev. **15**:631–646. http://dx.doi.org/10.1128/CMR.15.4.631-646.2002.
2. **Keim P, Johansson A, Wagner DM.** 2007. Molecular epidemiology, evolution, and ecology of *Francisella*. Ann. N. Y. Acad. Sci. **1105**:30–66. http://dx.doi.org/10.1196/annals.1409.011.
3. **Dennis DT, Inglesby TV, Henderson DA, Bartlett JG, Ascher MS, Eitzen E, Fine AD, Friedlander AM, Hauer J, Layton M, Lillibridge SR, McDade JE, Osterholm MT, O'Toole T, Parker G, Perl TM, Russell PK, Tonat K.** 2001. Tularemia as a biological weapon: medical and public health management. JAMA **285**:2763–2773. http://dx.doi.org/10.1001/jama.285.21.2763.
4. **Mikalsen J, Olsen AB, Rudra H, Moldal T, Lund H, Djønne B, Bergh O, Colquhoun DJ.** 2009. Virulence and pathogenicity of *Francisella philomi-*

ragia subsp. noatunensis for Atlantic cod, *Gadus morhua* L., and laboratory mice. J. Fish Dis. **32:**377–381. http://dx.doi.org/10.1111/j.1365-2761.2008.00987.x.
5. **Colquhoun DJ, Duodu S.** 2011. *Francisella* infections in farmed and wild aquatic organisms. Vet. Res. **42:**47. http://dx.doi.org/10.1186/1297-9716-42-47.
6. **Kamaishi T, Fukuda Y, Nishiyama M, Kawakami M, Matsuyama T, Yoshinaga T, Oseko N.** 2005. Identification and pathogenicity of intracellular *Francisella* bacterium in three-line grunt *Parapristipoma trilineatum*. Fish Pathol. **40:**67–71. http://dx.doi.org/10.3147/jsfp.40.67.
7. **Mauel MJ, Miller DL, Styer E, Pouder DB, Yanong RP, Goodwin AE, Schwedler TE.** 2005. Occurrence of piscirickettsiosis-like syndrome in tilapia in the continental United States. J. Vet. Diagn. Invest. **17:**601–605. http://dx.doi.org/10.1177/104063870501700616.
8. **Mauel MJ, Soto E, Moralis JA, Hawke J.** 2007. A piscirickettsiosis-like syndrome in cultured Nile tilapia in Latin America with *Francisella* spp. as the pathogenic agent. J. Aquat. Anim. Health **19:**27–34. http://dx.doi.org/10.1577/H06-025.1.
9. **Jeffery KR, Stone D, Feist SW, Verner-Jeffreys DW.** 2010. An outbreak of disease caused by *Francisella* sp. in Nile tilapia *Oreochromis niloticus* at a recirculation fish farm in the UK. Dis. Aquat. Organ. **91:**161–165. http://dx.doi.org/10.3354/dao02260.
10. **Birkbeck TH, Bordevik M, Frøystad MK, Baklien A.** 2007. Identification of *Francisella* sp. from Atlantic salmon, *Salmo salar* L., in Chile. J. Fish Dis. **30:**505–507. http://dx.doi.org/10.1111/j.1365-2761.2007.00837.x.
11. **Olsen AB, Mikalsen J, Rode M, Alfjorden A, Hoel E, Straum-Lie K, Haldorsen R, Colquhoun DJ.** 2006. A novel systemic granulomatous inflammatory disease in farmed Atlantic cod, *Gadus morhua* L., associated with a bacterium belonging to the genus *Francisella*. J. Fish Dis. **29:**307–311. http://dx.doi.org/10.1111/j.1365-2761.2006.00714.x.
12. **Nylund A, Ottem KF, Watanabe K, Karlsbakk E, Krossøy B.** 2006. *Francisella* sp. (Family *Francisellaceae*) causing mortality in Norwegian cod (*Gadus morhua*) farming. Arch. Microbiol. **185:**383–392. http://dx.doi.org/10.1007/s00203-006-0109-5.
13. **Jones RM, Nicas M, Hubbard A, Sylvester MD, Reingold A.** 2005. The infectious dose of *Francisella tularensis* (tularemia). Appl. Biosaf. **10:**227–239.
14. **Soto E, Fernandez D, Hawke JP.** 2009. Attenuation of the fish pathogen *Francisella* sp. by mutation of the iglC* gene. J. Aquat. Anim. Health **21:**140–149. http://dx.doi.org/10.1577/H08-056.1.
15. **Kamaishi T, Miwa S, Goto E, Matsuyama T, Oseko N.** 2010. Mass mortality of giant abalone *Haliotis gigantea* caused by a *Francisella* sp. bacterium. Dis. Aquat. Organ. **89:**145–154. http://dx.doi.org/10.3354/dao02188.
16. **Soto E, Hawke JP, Fernandez D, Morales JA.** 2009. *Francisella* sp., an emerging pathogen of tilapia, *Oreochromis niloticus* (L.), in Costa Rica. J. Fish Dis. **32:**713–722. http://dx.doi.org/10.1111/j.1365-2761.2009.01070.x.
17. **Golovliov I, Baranov V, Krocova Z, Kovarova H, Sjöstedt A.** 2003. An attenuated strain of the facultative intracellular bacterium *Francisella tularensis* can escape the phagosome of monocytic cells. Infect. Immun. **71:**5940–5950. http://dx.doi.org/10.1128/IAI.71.10.5940-5950.2003.
18. **Chong A, Celli J.** 2010. The *Francisella* intracellular life cycle: toward molecular mechanisms of intracellular survival and proliferation. Front. Microbiol. **1:**138 doi:http://dx.doi.org/10.3389/fmicb.2010.00138.
19. **Checroun C, Wehrly TD, Fischer ER, Hayes SF, Celli J.** 2006. Autophagy-mediated reentry of *Francisella tularensis* into the endocytic compartment after cytoplasmic replication. Proc. Natl. Acad. Sci. U. S. A. **103:**14578–14583. http://dx.doi.org/10.1073/pnas.0601838103.
20. **Soto E, Fernandez D, Thune R, Hawke JP.** 2010. Interaction of *Francisella asiatica* with tilapia (*Oreochromis niloticus*) innate immunity. Infect. Immun. **78:**2070–2078. http://dx.doi.org/10.1128/IAI.01308-09.
21. **Bakkemo KR, Mikkelsen H, Bordevik M, Torgersen J, Winther-Larsen HC, Vanberg C, Olsen R, Johansen LH, Seppola M.** 2011. Intracellular localisation and innate immune responses following Francisella noatunensis infection of Atlantic cod (Gadus morhua) macrophages. Fish Shellfish Immunol. **31:**993–1004. http://dx.doi.org/10.1016/j.fsi.2011.08.020.
22. **Furevik A, Pettersen EF, Colquhoun D, Wergeland HI.** 2011. The intracellular lifestyle of Francisella noatunensis in Atlantic cod (Gadus morhua L.) leucocytes. Fish Shellfish Immunol. **30:**488–494. http://dx.doi.org/10.1016/j.fsi.2010.11.019.
23. **Lyons CR, Wu TH.** 2007. Animal models of Francisella tularensis infection. Ann. N. Y. Acad. Sci. **1105:**238–265. http://dx.doi.org/10.1196/annals.1409.003.
24. **Cross AS, Calia FM, Edelman R.** 2007. From rabbits to humans: the contributions of Dr. Theodore E. Woodward to tularemia research. Clin. Infect. Dis. **45:**S61–S67. http://dx.doi.org/10.1086/518150.
25. **Pechous RD, McCarthy TR, Zahrt TC.** 2009. Working toward the future: insights into *Francisella tularensis* pathogenesis and vaccine development. Microbiol. Mol. Biol. Rev. **73:**684–711. http://dx.doi.org/10.1128/MMBR.00028-09.
26. **Hepburn MJ, Purcell BK, Lawler JV, Coyne SR, Petitt PL, Sellers KD, Norwood DA, Ulrich MP.** 2006. Live vaccine strain *Francisella tularensis* is detectable at the inoculation site but not in blood after vaccination against tularemia. Clin. Infect. Dis. **43:**711–716. http://dx.doi.org/10.1086/506348.
27. **Fuller CL, Brittingham KC, Hepburn MJ, Martin JW, Petitt PL, Pittman PR, Bavari S.** 2006. Dominance of human innate immune responses in primary *Francisella tularensis* live vaccine strain vaccination. J. Allergy Clin. Immunol. **117:**1186–1188. (Letter.) http://dx.doi.org/10.1016/j.jaci.2006.01.044.
28. **Soto E, Wiles J, Elzer P, Macaluso K, Hawke JP.** 2011. Attenuated *Francisella asiatica iglC* mutant induces protective immunity to francisellosis in tilapia. Vaccine **29:**593–598. http://dx.doi.org/10.1016/j.vaccine.2010.06.040.
29. **Ellingsen T, Inami M, Gjessing MC, Van Nieuwenhove K, Larsen R, Seppola M, Lund V, Schrøder MB.** 2011. *Francisella noatunensis* in Atlantic cod (*Gadus morhua* L.); waterborne transmission and immune responses. Fish Shellfish Immunol. **31:**326–333. http://dx.doi.org/10.1016/j.fsi.2011.05.021.
30. **Phelps HA, Neely MN.** 2005. Evolution of the zebrafish model: from development to immunity and infectious disease. Zebrafish **2:**87–103. http://dx.doi.org/10.1089/zeb.2005.2.87.
31. **Meijer AH, Spaink HP.** 2011. Host-pathogen interactions made transparent with the zebrafish model. Curr. Drug Targets **12:**1000–1017. http://dx.doi.org/10.2174/138945011795677809.
32. **Allen JP, Neely MN.** 2010. Trolling for the ideal model host: zebrafish take the bait. Future Microbiol. **5:**563–569. http://dx.doi.org/10.2217/fmb.10.24.
33. **Lam SH, Chua HL, Gong Z, Lam TJ, Sin YM.** 2004. Development and maturation of the immune system in zebrafish, Danio rerio: a gene expression profiling, in situ hybridization and immunological study. Dev. Comp. Immunol. **28:**9–28. http://dx.doi.org/10.1016/S0145-305X(03)00103-4.
34. **Herbomel P, Thisse B, Thisse C.** 1999. Ontogeny and behaviour of early macrophages in the zebrafish embryo. Development **126:**3735–3745.
35. **van der Sar AM, Musters RJ, van Eeden FJ, Appelmelk BJ, Vandenbroucke-Grauls CM, Bitter W.** 2003. Zebrafish embryos as a model host for the real time analysis of Salmonella typhimurium infections. Cell. Microbiol. **5:**601–611. http://dx.doi.org/10.1046/j.1462-5822.2003.00303.x.
36. **Vojtech LN, Sanders GE, Conway C, Ostland V, Hansen JD.** 2009. Host immune response and acute disease in a zebrafish model of *Francisella* pathogenesis. Infect. Immun. **77:**914–925. http://dx.doi.org/10.1128/IAI.01201-08.
37. **Brudal E, Winther-Larsen HC, Colquhoun DJ, Duodu S.** 2013. Evaluation of reference genes for reverse transcription quantitative PCR analyses of fish-pathogenic *Francisella* strains exposed to different growth conditions. BMC Res. Notes **6:**76. http://dx.doi.org/10.1186/1756-0500-6-76.
38. **Ellett F, Pase L, Hayman JW, Andrianopoulos A, Lieschke GJ.** 2011. *mpeg1* promoter transgenes direct macrophage-lineage expression in zebrafish. Blood **117:**e49–e56. http://dx.doi.org/10.1182/blood-2010-10-314120.
39. **Renshaw SA, Loynes CA, Trushell DM, Elworthy S, Ingham PW, Whyte MK.** 2006. A transgenic zebrafish model of neutrophilic inflammation. Blood **108:**3976–3978. http://dx.doi.org/10.1182/blood-2006-05-024075.
40. **Westerfield M.** 2000. The zebrafish book. A guide for the laboratory use of zebrafish (*Danio rerio*), 4th ed. University of Oregon Press, Eugene, OR.
41. **Matthews M, Varga ZM.** 2012. Anesthesia and euthanasia in zebrafish. ILAR J. **53:**192–204. http://dx.doi.org/10.1093/ilar.53.2.192.
42. **Schindelin J, Arganda-Carreras I, Frise E, Kaynig V, Longair M, Pietzsch T, Preibisch S, Rueden C, Saalfeld S, Schmid B, Tinevez JY, White DJ, Hartenstein V, Eliceiri K, Tomancak P, Cardona A.** 2012. Fiji: an open-source platform for biological-image analysis. Nat. Methods **9:**676–682. http://dx.doi.org/10.1038/nmeth.2019.
43. **van der Vaart M, Spaink HP, Meijer AH.** 2012. Pathogen recognition

and activation of the innate immune response in zebrafish. Adv. Hematol. **2012:**159807. http://dx.doi.org/10.1155/2012/159807.
44. **Zhang DC, Shao YQ, Huang YQ, Jiang SG.** 2005. Cloning, characterization and expression analysis of interleukin-10 from the zebrafish (*Danio rerio*). J. Biochem. Mol. Biol. **38:**571–576. http://dx.doi.org/10.5483/BMBRep.2005.38.5.571.
45. **Wang Z, Zhang S, Wang G.** 2008. Response of complement expression to challenge with lipopolysaccharide in embryos/larvae of zebrafish *Danio rerio*: acquisition of immunocompetent complement. Fish Shellfish Immunol. **25:**264–270. http://dx.doi.org/10.1016/j.fsi.2008.05.010.
46. **Igawa D, Sakai M, Savan R.** 2006. An unexpected discovery of two interferon gamma-like genes along with interleukin (IL)-22 and -26 from teleost: IL-22 and -26 genes have been described for the first time outside mammals. Mol. Immunol. **43:**999–1009. http://dx.doi.org/10.1016/j.molimm.2005.05.009.
47. **Altmann SM, Mellon MT, Johnson MC, Paw BH, Trede NS, Zon LI, Kim CH.** 2004. Cloning and characterization of an Mx gene and its corresponding promoter from the zebrafish, *Danio rerio*. Dev. Comp. Immunol. **28:**295–306. http://dx.doi.org/10.1016/j.dci.2003.09.001.
48. **Yoshimura A, Naka T, Kubo M.** 2007. SOCS proteins, cytokine signalling and immune regulation. Nat. Rev. Immunol. **7:**454–465. http://dx.doi.org/10.1038/nri2093.
49. **Dios S, Romero A, Chamorro R, Figueras A, Novoa B.** 2010. Effect of the temperature during antiviral immune response ontogeny in teleosts. Fish Shellfish Immunol. **29:**1019–1027. http://dx.doi.org/10.1016/j.fsi.2010.08.006.
50. **Tang R, Dodd A, Lai D, McNabb WC, Love DR.** 2007. Validation of zebrafish (*Danio rerio*) reference genes for quantitative real-time RT-PCR normalization. Acta Biochim. Biophys. Sin. (Shanghai) **39:**384–390. http://dx.doi.org/10.1111/j.1745-7270.2007.00283.x.
51. **McCurley AT, Callard GV.** 2008. Characterization of housekeeping genes in zebrafish: male-female differences and effects of tissue type, developmental stage and chemical treatment. BMC Mol. Biol. **9:**102. http://dx.doi.org/10.1186/1471-2199-9-102.
52. **Ottem KF, Nylund A, Isaksen TE, Karlsbakk E, Bergh Ø.** 2008. Occurrence of *Francisella piscicida* in farmed and wild Atlantic cod, *Gadus morhua* L., in Norway. J. Fish Dis. **31:**525–534. http://dx.doi.org/10.1111/j.1365-2761.2008.00930.x.
53. **Parsa KV, Butchar JP, Rajaram MV, Cremer TJ, Gunn JS, Schlesinger LS, Tridandapani S.** 2008. *Francisella* gains a survival advantage within mononuclear phagocytes by suppressing the host IFNgamma response. Mol. Immunol. **45:**3428–3437. http://dx.doi.org/10.1016/j.molimm.2008.04.006.
54. **Colucci-Guyon E, Tinevez JY, Renshaw SA, Herbomel P.** 2011. Strategies of professional phagocytes in vivo: unlike macrophages, neutrophils engulf only surface-associated microbes. J. Cell Sci. **124:**3053–3059. http://dx.doi.org/10.1242/jcs.082792.
55. **Kanwal Z, Zakrzewska A, den Hertog J, Spaink HP, Schaaf MJM, Meijer AM.** 2013. Deficiency in hematopoietic phosphatase ptpn6/Shp1 hyperactivates the innate immune system and impairs control of bacterial infections in zebrafish embryos. J. Immunol. **190:**1631–1645. http://dx.doi.org/10.4049/jimmunol.1200551.
56. **Gjessing MC, Inami M, Weli SC, Ellingsen T, Falk K, Koppang EO, Kvellestad A.** 2011. Presence and interaction of inflammatory cells in the spleen of Atlantic cod, *Gadus morhua* L., infected with *Francisella noatunensis*. J. Fish Dis. **34:**687–699. http://dx.doi.org/10.1111/j.1365-2761.2011.01284.x.
57. **Mikalsen J, Olsen AB, Tengs T, Colquhoun DJ.** 2007. *Francisella philomiragia* subsp. *noatunensis* subsp. nov., isolated from farmed Atlantic cod (*Gadus morhua* L.). Int. J. Syst. Evol. Microbiol. **57:**1960–1965. http://dx.doi.org/10.1099/ijs.0.64765-0.
58. **Davis JM, Clay H, Lewis JL, Ghori N, Herbomel P, Ramakrishnan L.** 2002. Real-time visualization of mycobacterium-macrophage interactions leading to initiation of granuloma formation in zebrafish embryos. Immunity **17:**693–702. http://dx.doi.org/10.1016/S1074-7613(02)00475-2.
59. **Ludwig M, Palha N, Torhy C, Briolat V, Colucci-Guyon E, Bremont M, Herbomel P, Boudinot P, Levraud JP.** 2011. Whole-body analysis of a viral infection: vascular endothelium is a primary target of infectious hematopoietic necrosis virus in zebrafish larvae. PLoS Pathog. **7:**e1001269. http://dx.doi.org/10.1371/journal.ppat.1001269.
60. **Cowley SC, Gray CJ, Nano FE.** 2000. Isolation and characterization of *Francisella novicida* mutants defective in lipopolysaccharide biosynthesis. FEMS Microbiol. Lett. **182:**63–67. http://dx.doi.org/10.1111/j.1574-6968.2000.tb08874.x.
61. **Benard EL, van der Sar AM, Ellett F, Lieschke GJ, Spaink HP, Meijer AH.** 2012. Infection of zebrafish embryos with intracellular bacterial pathogens. J. Vis. Exp. **2012:**e3781. http://dx.doi.org/10.3791/3781.
62. **Clemens DL, Lee BY, Horwitz MA.** 2004. Virulent and avirulent strains of *Francisella tularensis* prevent acidification and maturation of their phagosomes and escape into the cytoplasm in human macrophages. Infect. Immun. **72:**3204–3217. http://dx.doi.org/10.1128/IAI.72.6.3204-3217.2004.
63. **Hall JD, Woolard MD, Gunn BM, Craven RR, Taft-Benz S, Frelinger JA, Kawula TH.** 2008. Infected-host-cell repertoire and cellular response in the lung following inhalation of *Francisella tularensis* Schu S4, LVS, or U112. Infect. Immun. **76:**5843–5852. http://dx.doi.org/10.1128/IAI.01176-08.
64. **Dixon G, Elks PM, Loynes CA, Whyte MK, Renshaw SA.** 2012. A method for the in vivo measurement of zebrafish tissue neutrophil lifespan. ISRN Hematol. **2012:**915868. http://dx.doi.org/10.5402/2012/915868.
65. **Brannon MK, Davis JM, Mathias JR, Hall CJ, Emerson JC, Crosier PS, Huttenlocher A, Ramakrishnan L, Moskowitz SM.** 2009. *Pseudomonas aeruginosa* type III secretion system interacts with phagocytes to modulate systemic infection of zebrafish embryos. Cell. Microbiol. **11:**755–768. http://dx.doi.org/10.1111/j.1462-5822.2009.01288.x.
66. **Couper KN, Blount DG, Riley EM.** 2008. IL-10: the master regulator of immunity to infection. J. Immunol. **180:**5771–5777.
67. **Fortier AH, Polsinelli T, Green SJ, Nacy CA.** 1992. Activation of macrophages for destruction of *Francisella tularensis*: identification of cytokines, effector cells, and effector molecules. Infect. Immun. **60:**817–825.
68. **Aktan F.** 2004. iNOS-mediated nitric oxide production and its regulation. Life Sci. **75:**639–653. http://dx.doi.org/10.1016/j.lfs.2003.10.042.
69. **Wang T, Gorgoglione B, Maehr T, Holland JW, Vecino JL, Wadsworth S, Secombes CJ.** 2011. Fish suppressors of cytokine signaling (SOCS): gene discovery, modulation of expression and function. J. Signal Transduct. **2011:**905813. http://dx.doi.org/10.1155/2011/905813.
70. **Veneman WJ, Stockhammer OW, de Boer L, Zaat SA, Meijer AH, Spaink HP.** 2013. A zebrafish high throughput screening system used for *Staphylococcus epidermidis* infection marker discovery. BMC Genomics **14:**255. http://dx.doi.org/10.1186/1471-2164-14-255.